National Physical Laboratory

NPL Report ENG 49

Acoustic gas thermometry: models and corrections for argon from 90 K to 1500 K

GAVIN SUTTON

OCTOBER 2014

National Measurement System

Acoustic gas thermometry: models and corrections for argon from 90 K to 1500 K

Gavin Sutton

Engineering Measurement Division

ABSTRACT

This NPL report describes the models and corrections required for high precision acoustic gas thermometry using argon gas as the thermometric fluid over the temperature range 90 K < T < 1500 K. Where corrections require a specific geometry and or resonator material, it is assumed that the measurements are performed using a quasi-spherical acoustic resonator made of copper tuned to the radial acoustic modes.

© Queen's Printer and Controller of HMSO, 2014

ISSN 1754-2987

National Physical Laboratory

Hampton Road, Teddington, Middlesex, TW11 0LW

Extracts from this report may be reproduced provided the source is acknowledged and the extract is not taken out of context.

Approved on behalf of NPLML by Stephanie Bell, Assistant Knowledge Leader, Engineering Measurement Division.

Contents

1. INTRODUCTION

To second order in pressure, the speed of sound can be written as [1]:

$$u^2(T,p) = \frac{\gamma_0 RT}{M}(1 + A_1 p + A_2 p^2) \tag{1}$$

Where:

γ_0 is the ratio of specific heats C_p/C_v in the limit of zero pressure.
R is the molar gas constant.
T is the temperature.
M is the molar mass of the gas.
p is the pressure.

and $$A_1 = \frac{\beta}{RT} \quad , \quad A_2 = \frac{\phi}{(RT)^2} = \frac{L - B\beta}{(RT)^2} \tag{2}$$

β and ϕ are known as the second and third acoustic virial coefficients respectively.

with $$\beta = 2B + 2(\gamma_0 - 1)T\frac{dB}{dT} + \frac{(\gamma_0 - 1)^2}{\gamma_0}T^2\frac{d^2B}{dT^2} \tag{3a}$$

and $$L = \left[B + (2\gamma_0 - 1)T\frac{dB}{dT} + (\gamma_0 - 1)T^2\frac{d^2B}{dT^2}\right]^2\left(\frac{\gamma_0 - 1}{\gamma_0}\right) + \left(\frac{1 + 2\gamma_0}{\gamma_0}\right)C + \left(\frac{\gamma_0^2 - 1}{\gamma_0}\right)T\frac{dC}{dT} + \frac{(\gamma_0 - 1)^2}{2\gamma_0}T^2\frac{d^2C}{dT^2} \tag{3b}$$

In these expressions, B and C are the *second* and *third density virial coefficients*.

In this report, we start by defining expressions to facilitate the evaluation of the *speed of sound* in argon (Equation 1): the *second* and *third density virial coefficients*, their first and second derivatives with respect to T and the *second* and *third acoustic virial coefficients*. We continue by developing expressions for the thermophysical properties and perturbations to the resonance frequencies of a quasi-spherical acoustic resonator. We conclude with expressions for the duct, shape and transducers perturbations. Unless otherwise stated, all expressions are defined and have been tested over the temperature interval 90 K to 1500 K and, where appropriate, over the pressure range from 0 kPa to 1000 kPa.

2. SECOND DENSITY VIRIAL COEFFICIENT: B [$cm^3 mol^{-1}$]

We take values for the *second density virial coefficient* of argon, B from *Moldover et al* [2] reproduced in Appendix 1. Figure 1 shows a plot of this and a comparison with that of REFPROP [4, 5] – the agreement between the two is excellent. The Labview VI: *B argon 2014.vi* that calculates the value of $B(T)$ via cubic spline interpolation is also shown.

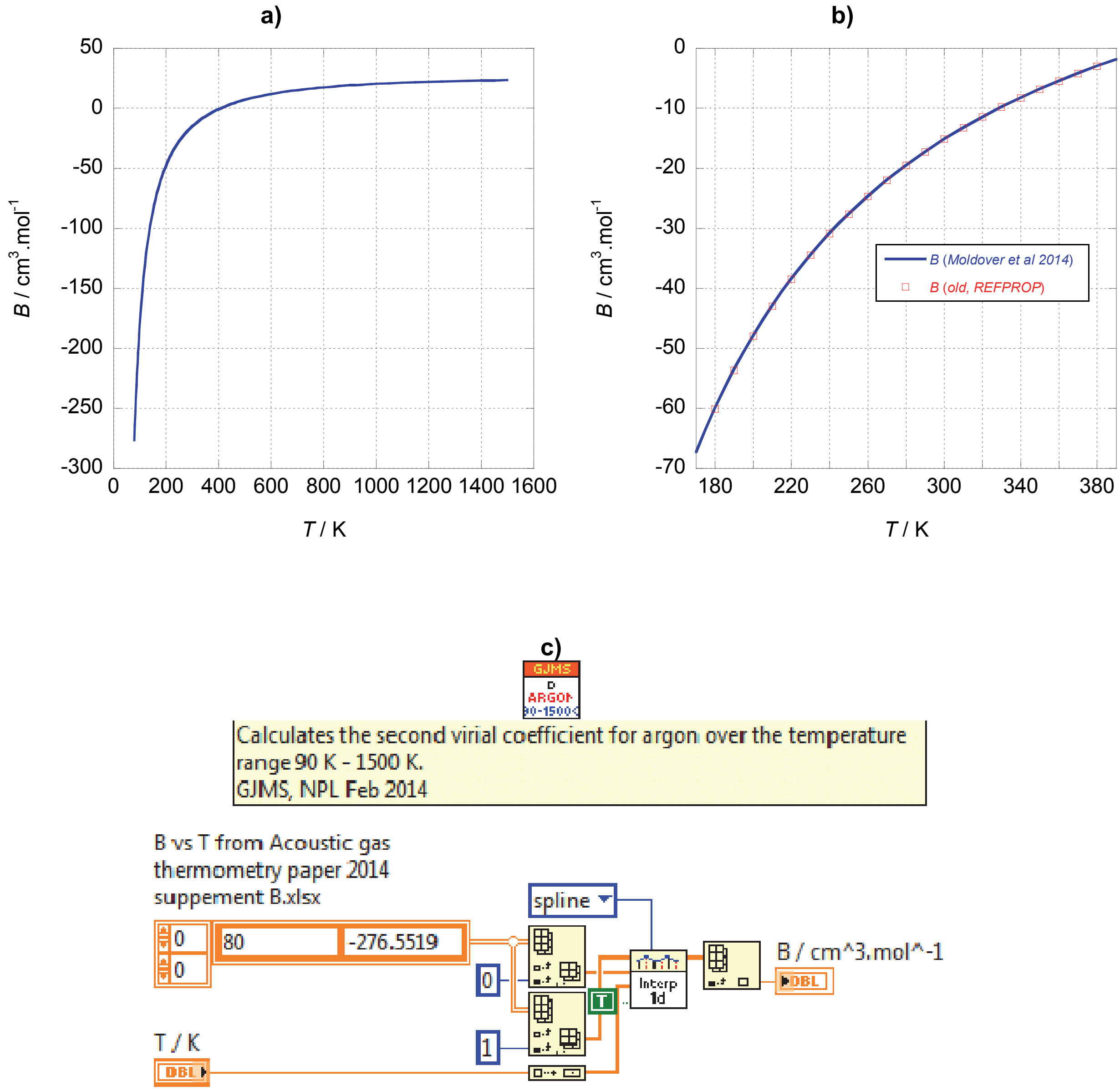

Figure 1 2[nd] *density virial coefficient* of argon, B : a) New data from *Moldover et al* [2], b) Comparison with REFPROP [4, 5] and c) Labview VI: *B argon 2014.vi*

3. FIRST DERIVATIVE OF THE SECOND DENSITY VIRIAL COEFFICIENT: dB/dT [cm^{3}mol^{-1}K^{-1}]

We calculate the numerical derivative of $B(T)$ with respect to T using:

$$\frac{\mathrm{d}B(T)}{\mathrm{d}T} = \frac{B(T+\Delta T) - B(T-\Delta T)}{2\Delta T} \tag{4}$$

With $\Delta T = 0.1$ K. Reducing ΔT further has negligible effect. Figure 2 shows a plot of $\mathrm{d}B/\mathrm{d}T$ for argon and a comparison with that from REFPROP [4, 5] – the agreement between the two is excellent. The Labview VI: *dBdT argon 2014.vi* that calculates it is also shown.

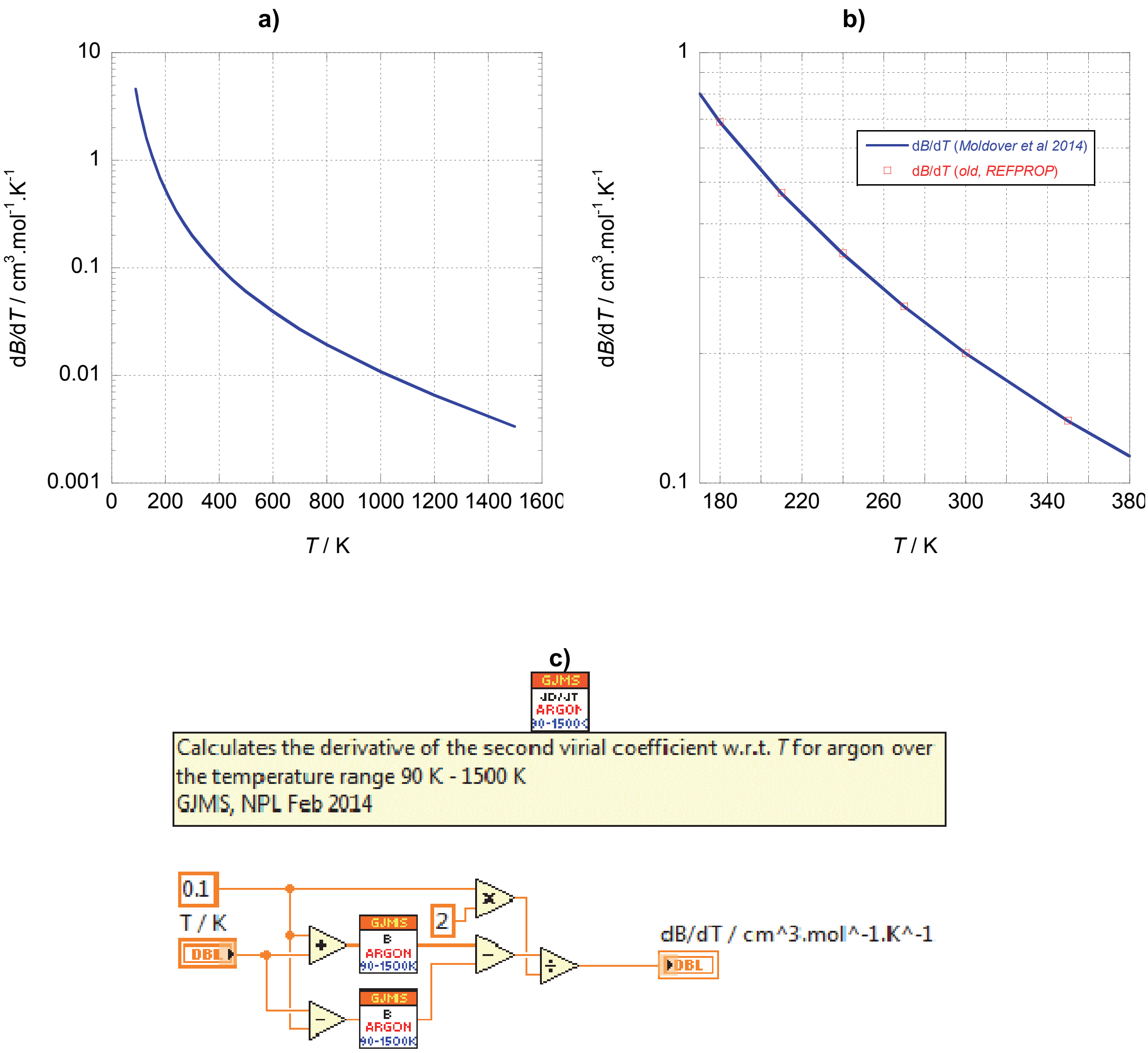

Figure 2 $\mathrm{d}B/\mathrm{d}T$ for argon: a) New data from *Moldover et al* [2], b) Comparison with REFPROP [4, 5] and c) Labview VI: *dBdT argon 2014.vi*

4. SECOND DERIVATIVE OF THE SECOND DENSITY VIRIAL COEFFICIENT: $\mathrm{d}^2B/\mathrm{d}T^2$ [$\mathrm{cm}^3\mathrm{mol}^{-1}\mathrm{K}^{-2}$]

We calculate the numerical second derivative of $B(T)$ with respect to T using:

$$\frac{\mathrm{d}^2B(T)}{\mathrm{d}T^2} = \frac{\frac{\mathrm{d}B(T+\Delta T)}{\mathrm{d}T} - \frac{\mathrm{d}B(T-\Delta T)}{\mathrm{d}T}}{2\Delta T} \qquad (5)$$

With $\Delta T = 0.1$ K. Reducing it further has negligible effect. Figure 3 shows a plot of $\mathrm{d}^2B/\mathrm{d}T^2$ for argon and a comparison with that from REFPROP [4, 5] – the agreement between the two is excellent. The Labview VI: *d2BdT2 argon 2014.vi* that calculates it is also shown.

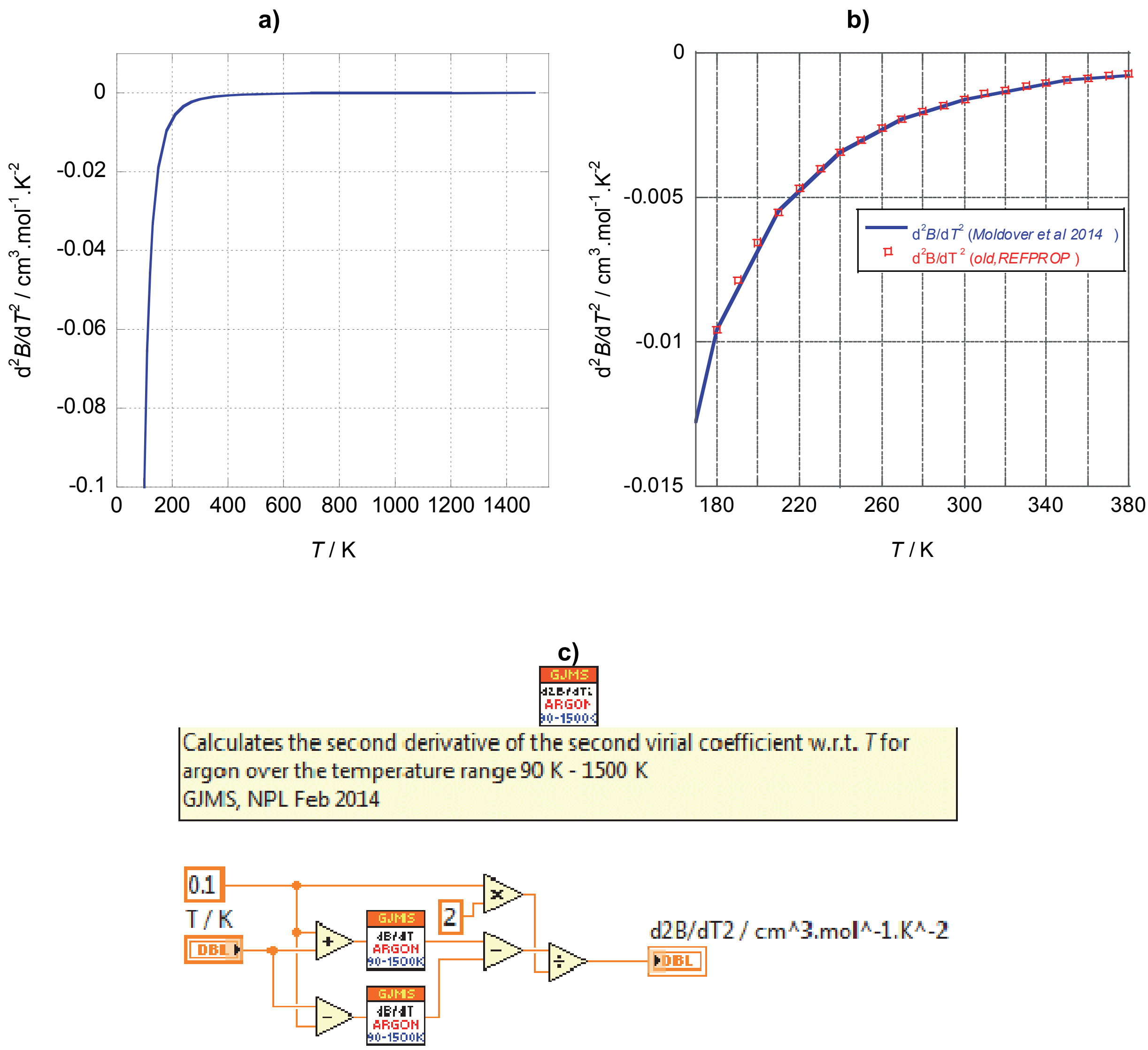

Figure 3 $\mathrm{d}^2B/\mathrm{d}T^2$ for argon: a) New data from *Moldover et al* [2], b) Comparison with REFPROP [4, 5] and c) Labview VI: d2*BdT2 argon 2014.vi*

5. THIRD DENSITY VIRIAL COEFFICIENT: C [cm^{6}mol^{-2}]

Following the recommendations given by *Moldover et al* [2], we make use of Equation 21 and the supplementary information provided in *Jäger et al* [3] to calculate the third density virial coefficient of argon. The equation to calculate $C(T)$ is:

$$C(T) = \sum_{k=-9}^{3} c_{3,k} T^{*k} + c_{3,0.5}\sqrt{T^*} + \frac{c_{3,-0.5}}{\sqrt{T^*}} \tag{6}$$

Where $T^* = T/(1000\text{ K})$ and Appendix III gives the coefficients $c_{3,k}$. Figure 4 shows a plot of this and the Labview VI: *C argon 2014.vi* that calculates it. We see good agreement with the value determined from REFPROP [4, 5].

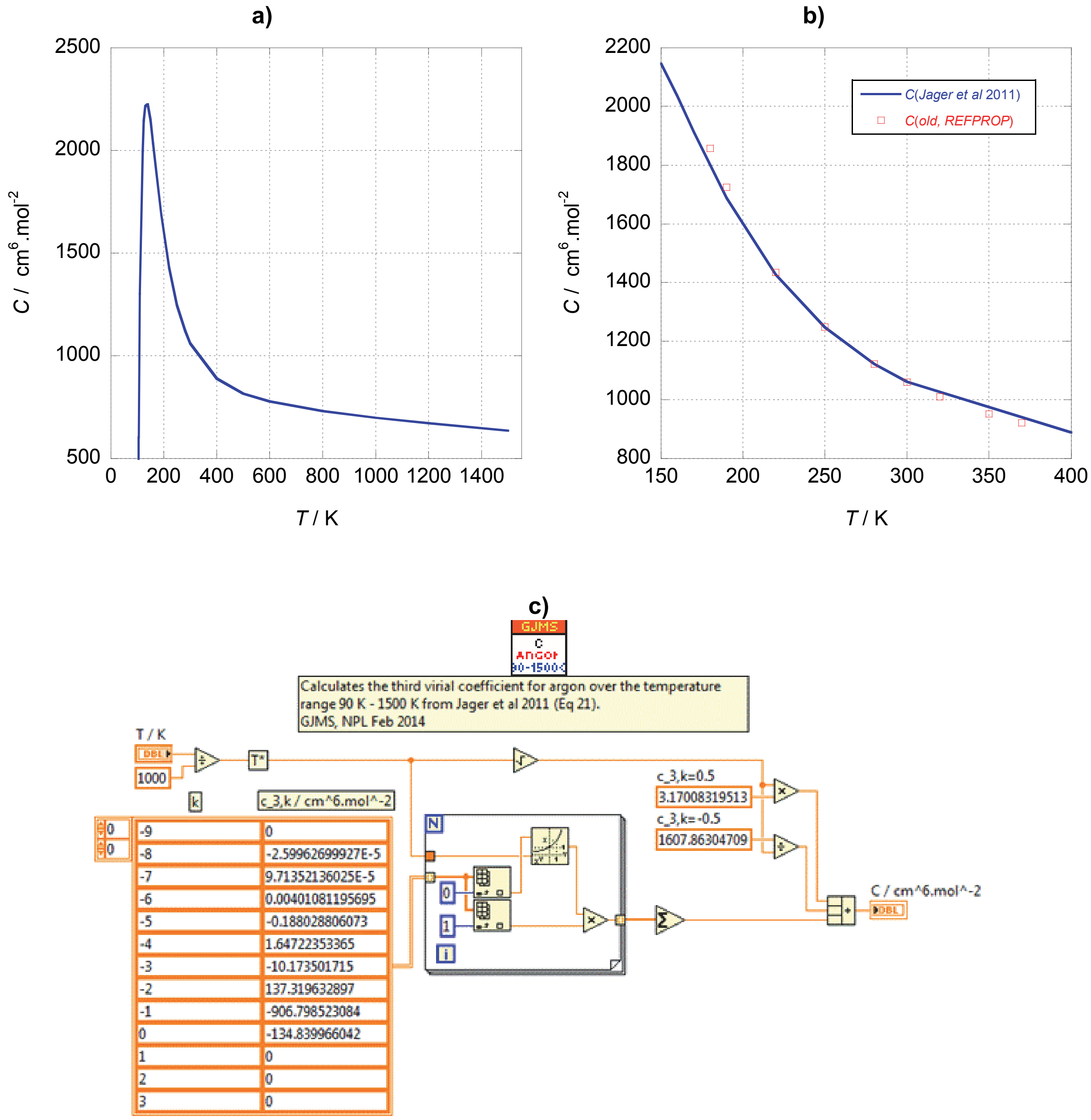

Figure 4 Third density virial coefficient for argon: a) new calculation from *Jäger et al* (2011) [3], b) comparison of this with the old determination from REFPROP [4, 5] and c) Labview VI: *C argon 2014.vi.*

6. FIRST DERIVATIVE OF THE THIRD DENSITY VIRIAL COEFFICIENT: dC/dT [cm^{6}mol^{-2}K^{-1}]

We calculate the numerical derivative of $C(T)$ with respect to T using:

$$\frac{\mathrm{d}C(T)}{\mathrm{d}T} = \frac{C(T+\Delta T) - C(T-\Delta T)}{2\Delta T} \tag{7}$$

With $\Delta T = 0.1$ K. Reducing ΔT further has negligible effect. Figure 5 shows a plot of $\mathrm{d}C/\mathrm{d}T$ for argon and the Labview VI: *dCdT argon 2014.vi* that calculates it. We see that $\mathrm{d}C/\mathrm{d}T$ calculated with REFPROP [4, 5] departs from the new determination at low temperatures – this is perhaps, not surprising, since we approach a sharp minima in $\mathrm{d}C/\mathrm{d}T$ around T = 165 K.

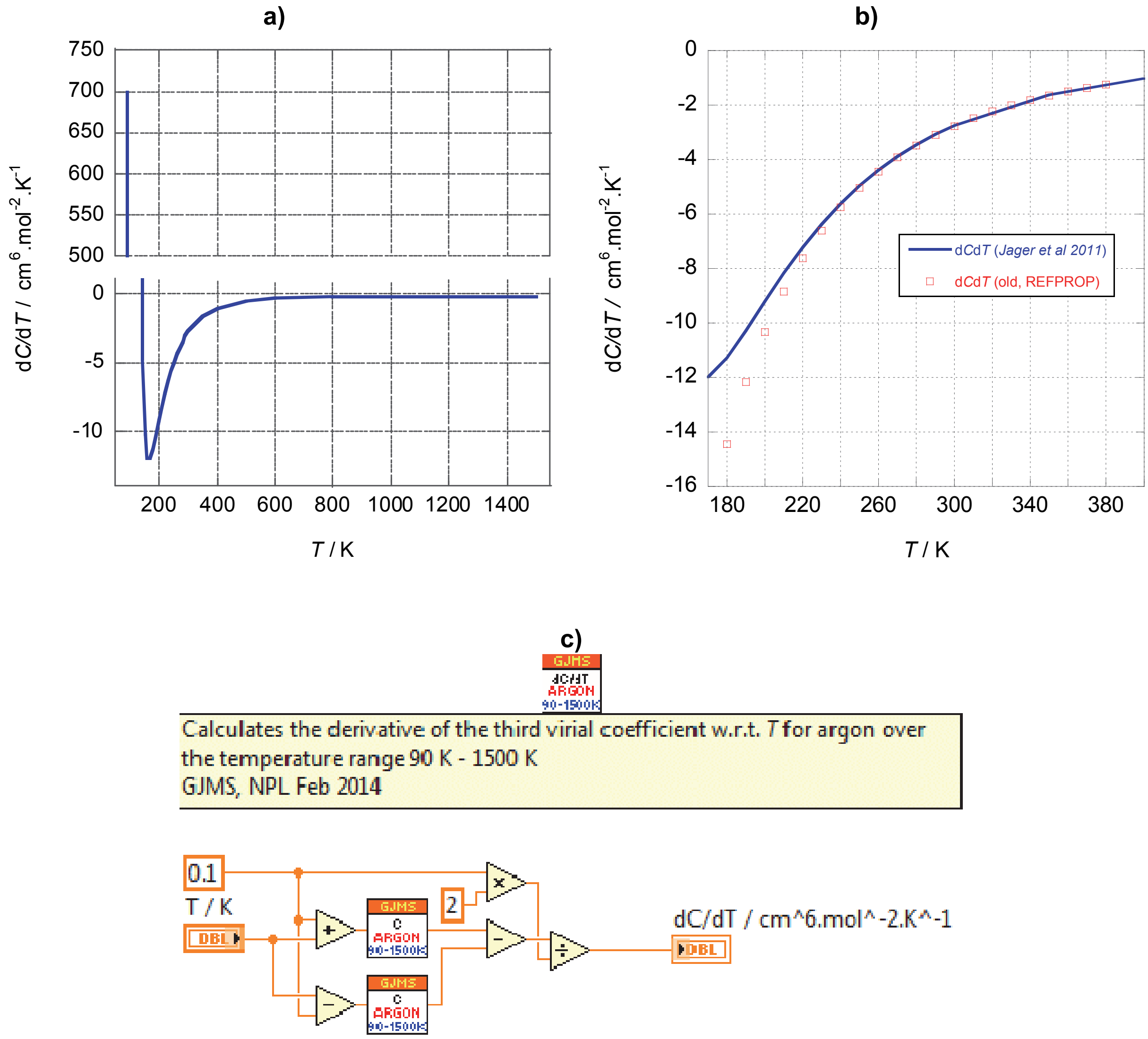

Figure 5 $\mathrm{d}C/\mathrm{d}T$ for argon: a) new calculation from *Jäger et al 2011*, b) comparison of this with the old determination from REFPROP [4, 5] and c) Labview VI: *dCdT argon 2014.vi.*

7. SECOND DERIVATIVE OF THE THIRD DENSITY VIRIAL COEFFICIENT: d^2C/dT^2 [$cm^6mol^{-2}K^{-2}$]

We calculate the numerical second derivative of $C(T)$ with respect to T using:

$$\frac{\mathrm{d}^2C(T)}{\mathrm{d}C^2} = \frac{\frac{\mathrm{d}C(T+\Delta T)}{\mathrm{d}T} - \frac{\mathrm{d}C(T-\Delta T)}{\mathrm{d}T}}{2\Delta T} \tag{8}$$

With $\Delta T = 0.1$ K. Reducing it further has negligible effect. Figure 6 shows a plot of this and the Labview VI: *d2CdT2 argon 2014.vi* that calculates it. We see that $\mathrm{d}^2C/\mathrm{d}T^2$ calculated with REFPROP [4, 5] departs from the new determination at low temperatures.

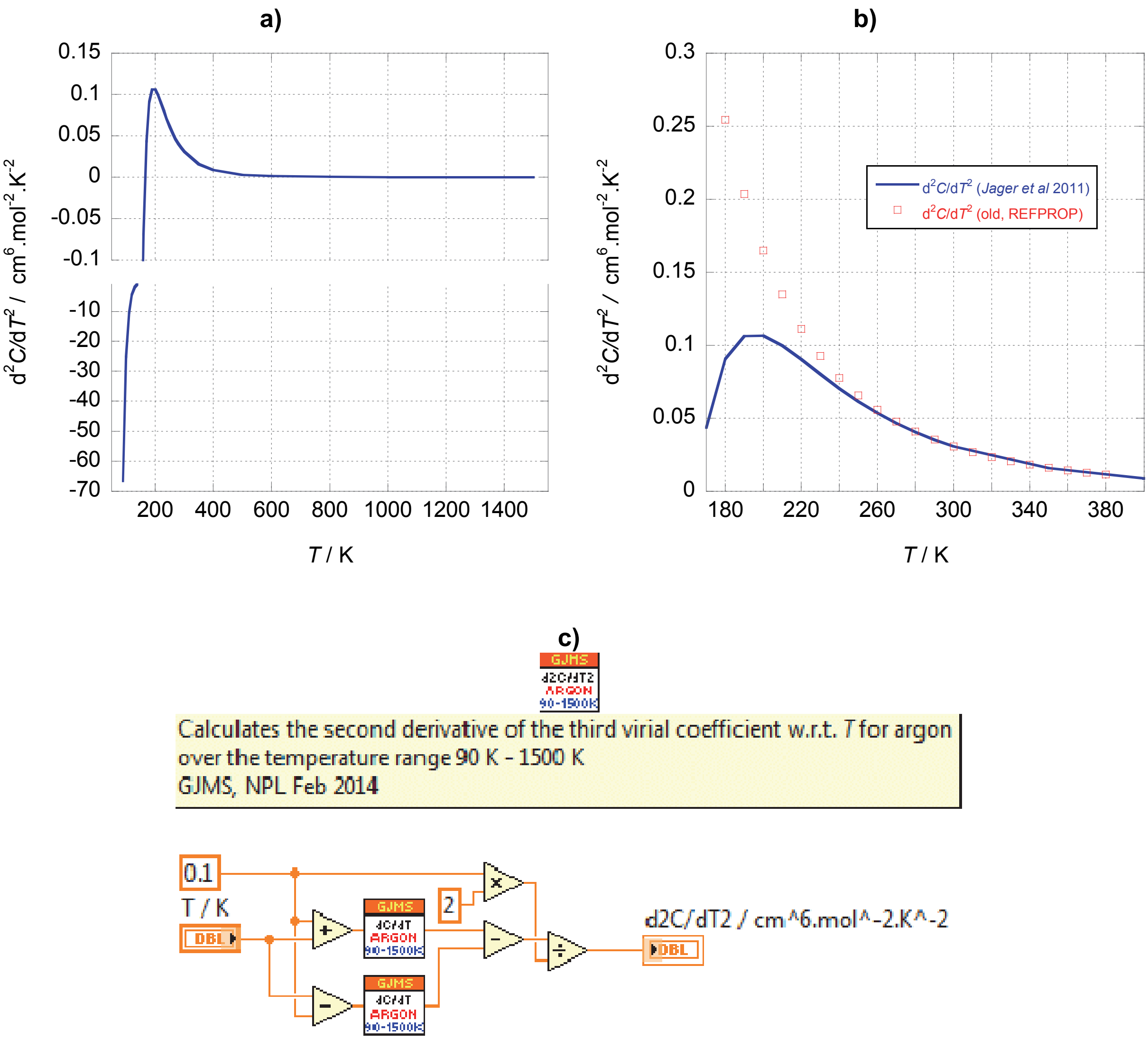

Figure 6 $\mathrm{d}^2C/\mathrm{d}T^2$ for argon: a) new calculation from *Jäger et al 2011*, b) comparison of this with the old determination from REFPROP [4, 5] and c) Labview VI: *d2CdT2 argon 2014.vi.*

8. SECOND ACOUSTIC VIRIAL COEFFICIENT: β [cm^{3}mol^{-1}]

The second acoustic virial coefficient, β is defined in terms of the second density virial coefficient, B and its derivatives as:

$$\beta = 2B + 2(\gamma_0 - 1)T\frac{\mathrm{d}B}{\mathrm{d}T} + \frac{(\gamma_0 - 1)^2}{\gamma_0}T^2\frac{\mathrm{d}^2B}{\mathrm{d}T^2} \tag{9}$$

We calculate $\beta(T)$ using cubic spline interpolation on the data from *Moldover et al* [2] given in Appendix 1 and compare this with that calculated with REFPROP [4, 5]. We note that calculating β using Equation 9 gives the same result as that given in Appendix 1. Figure 7 shows this and the Labview VI: *Beta argon 2014.vi* used to calculate it.

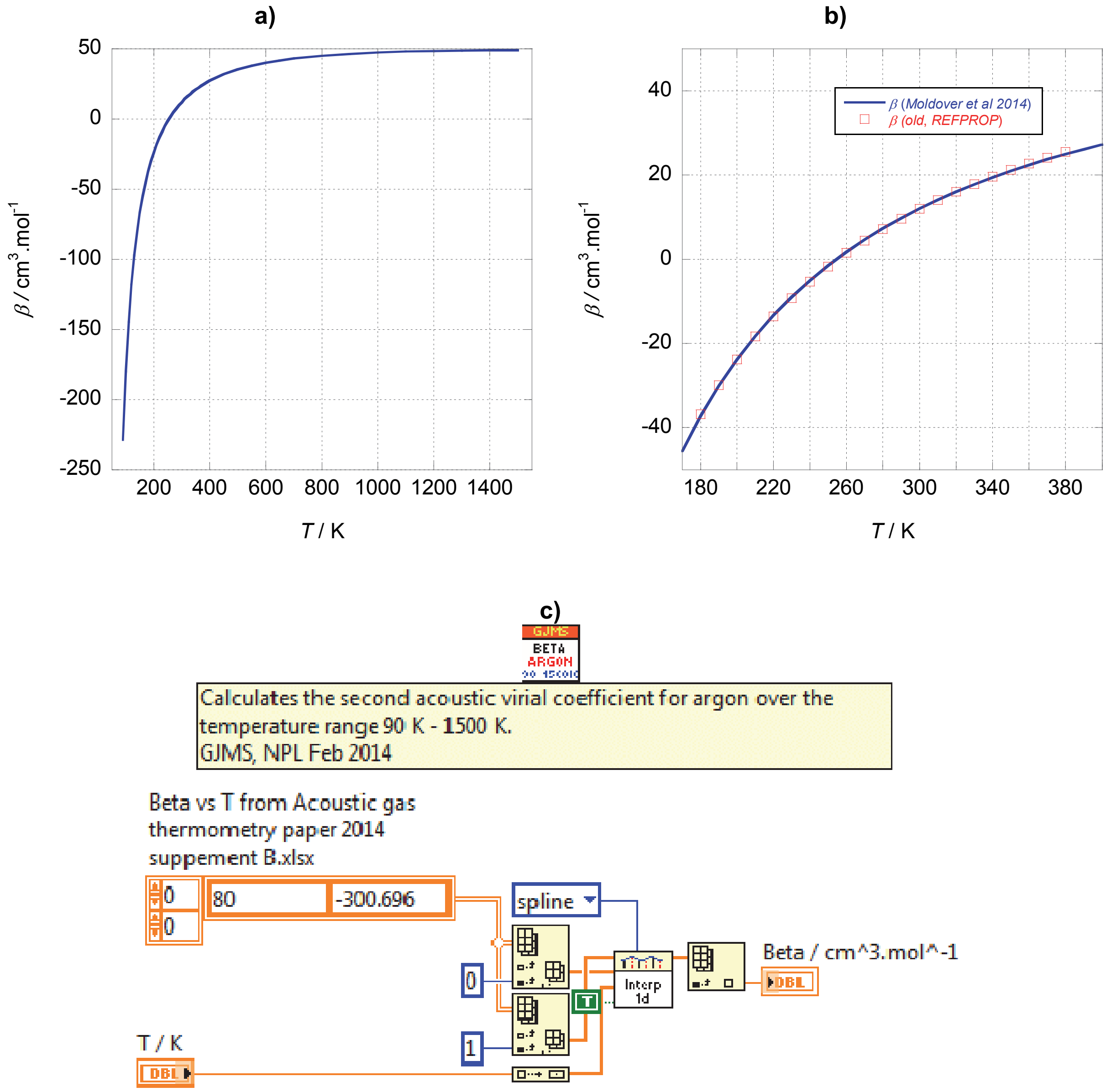

Figure 7 β for argon: a) new calculation from *Moldover et al* [2], b) comparison of this with the old determination from REFPROP [4, 5] and c) Labview VI: *Beta argon 2014.vi.*

9. THIRD ACOUSTIC VIRIAL COEFFICIENT: ϕ [cm^{6}mol^{-2}]

The third acoustic virial coefficient, ϕ is defined in terms of the second acoustic virial coefficient, β, the second and third density virial coefficients, B and C, and their derivatives as:

$$\phi = L - B\beta \tag{10a}$$

$$\begin{aligned} L = {} & \left[B + (2\gamma_0 - 1)T\frac{\mathrm{d}B}{\mathrm{d}T} + (\gamma_0 - 1)T^2\frac{\mathrm{d}^2B}{\mathrm{d}T^2}\right]^2\left(\frac{\gamma_0 - 1}{\gamma_0}\right) \\ & + \left(\frac{1 + 2\gamma_0}{\gamma_0}\right)C + \left(\frac{\gamma_0^2 - 1}{\gamma_0}\right)T\frac{\mathrm{d}C}{\mathrm{d}T} \\ & + \frac{(\gamma_0 - 1)^2}{2\gamma_0}T^2\frac{\mathrm{d}^2C}{\mathrm{d}T^2} \end{aligned} \tag{10b}$$

We calculate $\phi(T)$ using Equation 10 and compare this with that calculated with REFPROP [4, 5]. Figure 8 shows this and the Labview VI: *Phi argon 2014.vi* used to calculate it. We see reasonable agreement between this new determination and that of REFPROP [4, 5]. At lower temperatures, a large variability in $\phi(T)$ between authors is reported. This is discussed further in Appendix IV.

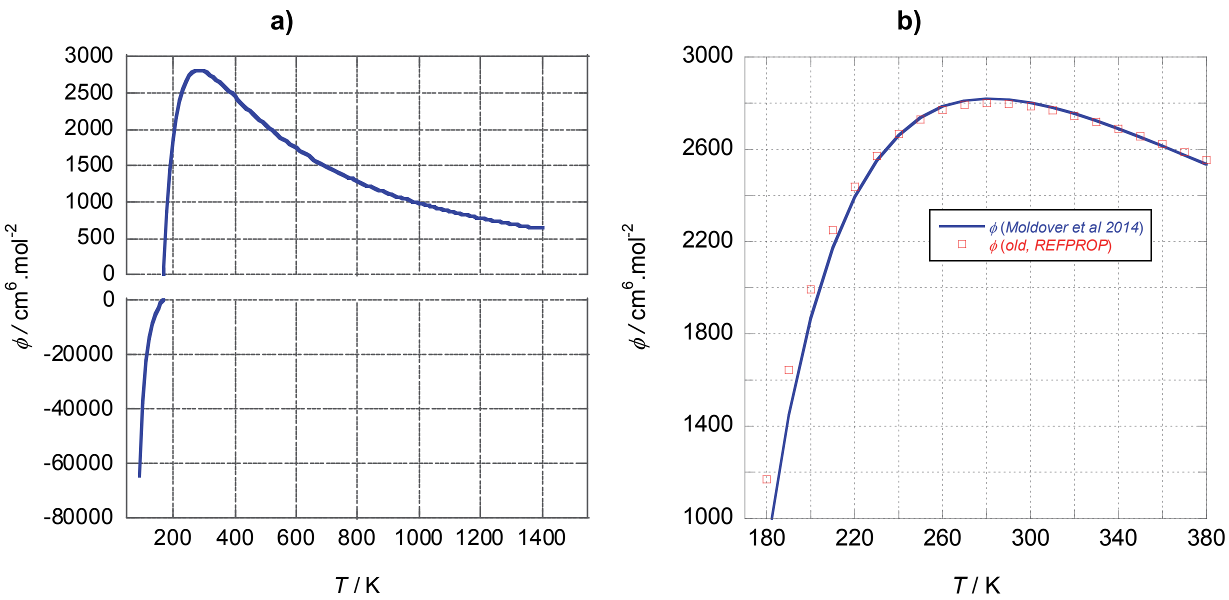

c)

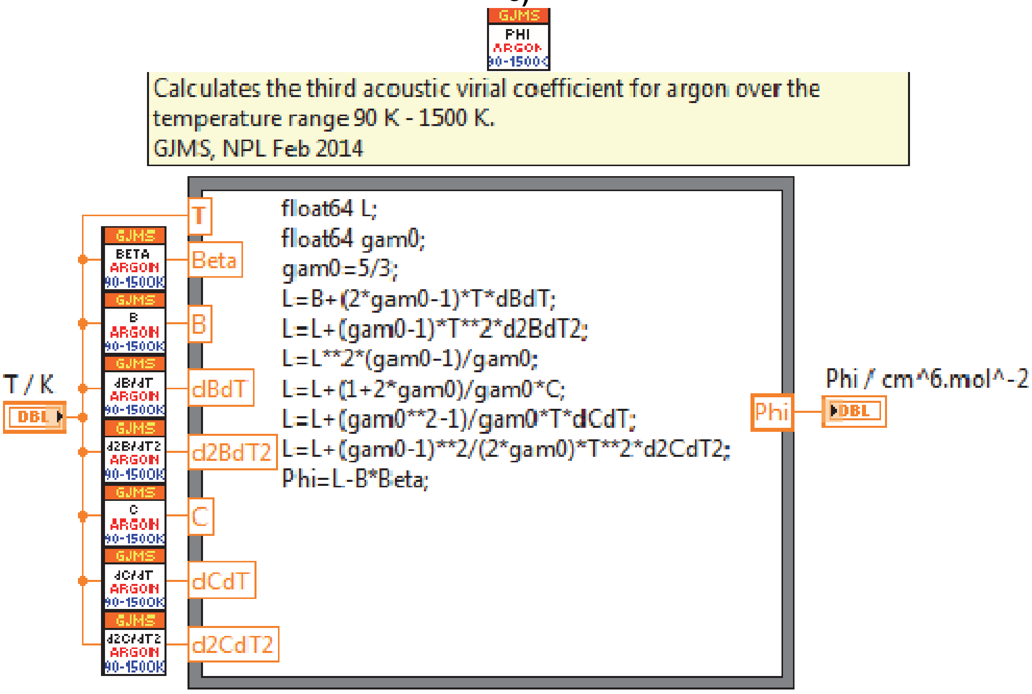

Figure 8 ϕ for argon: a) new calculation from *Moldover et al* [2], b) comparison of this with the old determination from REFPROP [4, 5] and c) Labview VI: *Phi argon 2014.vi.*

10. SPEED OF SOUND: u [MS^{-1}]

To second order in pressure, the *speed of sound squared* can be written as:

$$u^2(T,p) = \frac{\gamma_0 RT}{M}(1 + A_1 p + A_2 p^2) \tag{11}$$

Where β and ϕ are the second and third acoustic virial coefficients respectively.
Re-arranging Equation 11, we may write:

$$\frac{u^2(T,p)}{u_0^2} = \frac{u^2(T,p)}{\frac{\gamma_0 RT}{M}} = (1 + A_1 p + A_2 p^2) \tag{12}$$

Figure 9 shows the values of $u(T,p)$ versus T, the fractional difference from $u(T,0)$ and the values of $A_1 p$ and $A_2 p^2$ for argon for various pressures. The Labview VI: *U 2nd argon 2014.vi* is also shown.

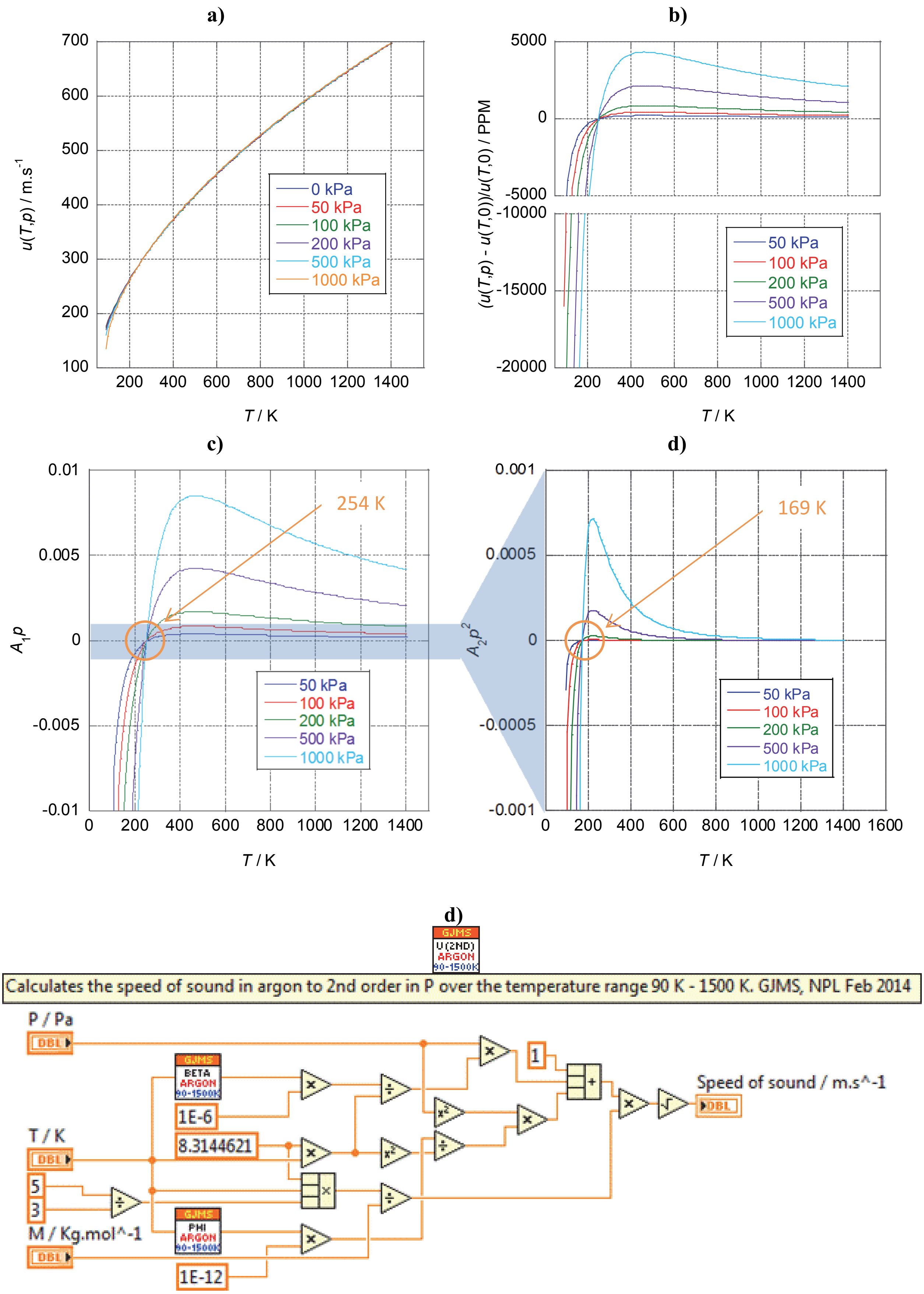

Figure 9 Speed of sound in argon: a) $u(T,p)$ versus T for various pressures, b) fractional difference from $u(T,0)$, fractional contributions to $u^2(T,p)$ in terms of c) p and d) $p^2$and d) the Labview VI: *U 2nd argon 2014.vi*

11. EIGENVALUE OF THE (n, s) MODE FOR AN IDEAL SPHERE: Z_{ns}

The acoustic eigenvalue for a perfect sphere Z_{ns}, is given by the s^{th} zero of the derivative of the *Spherical Bessel Function* of order n. It is used to determine the ideal resonance frequencies. Table 1 shows the eigenvalues up to order 8 and 10th zero. Where a '-' appears in the table, the software was unable to generate the value to sufficient accuracy (0.01 PPM). Figure 10 shows the Labview VI: *Calc Z 2014.vi*.

Table 1 Acoustic Eigenvalues Z_{ns} of a perfect sphere. $n = 0$ corresponds to the radial modes.

n	S = 1	s = 2	s = 3	s = 4	s = 5	s = 6	s = 7	s = 8	s = 9	s = 10
0	-	4.49340945	7.72525184	10.90412166	14.06619391	17.22075527	20.37130296	23.51945249	26.66605425	29.81159879
1	2.08157598	5.94036999	9.20584014	12.40444502	15.57923641	18.74264558	21.89969648	25.05282528	28.203361	31.35209172
2	3.34209365	7.28993230	10.61385504	13.84611188	17.04290219	20.22185656	23.39049018	26.55258922	29.71027992	-
3	4.51409965	8.58375495	11.97273003	15.24451382	18.46814777	21.66660692	24.85008531	-	-	-
4	5.64670362	9.84044604	13.29556386	16.60934590	19.86242396	23.08279562	-	-	-	-
5	6.75645633	11.07020687	14.59055216	17.94717953	21.23106830	-	-	-	-	-
6	7.85107768	12.27933398	15.86322182	19.26270994	-	-	-	-	-	-
7	8.93483887	13.47203035	17.11750573	20.55942813	-	-	-	-	-	-
8	10.01037074	14.65126281	18.35631834	21.84001207	-	-	-	-	-	-

a)

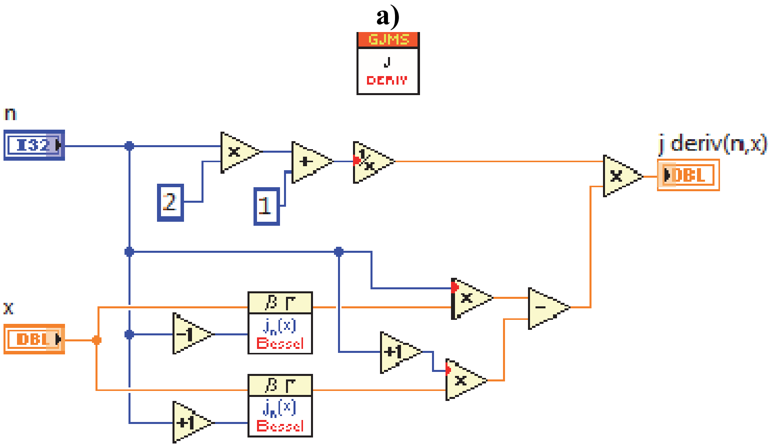

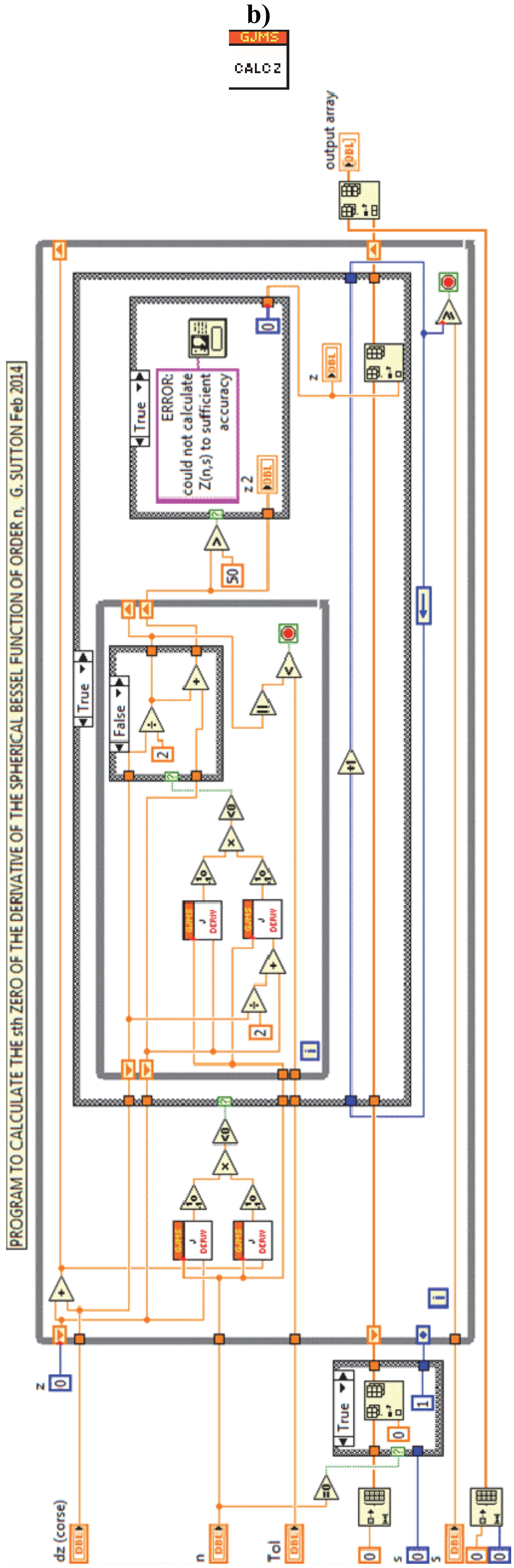

Figure 10 Labview VI: *Calc Z 2014.vi* that calculates the acoustic Eigenvalues for a perfect sphere Z_{ns} . The Labview VI: *J deriv.vi* need by this VI is given first.

12. RESONANCE FREQUENCIES FOR AN IDEAL SPHERE: *f*(*n*, *s*) [Hz]

The resonance frequencies of an ideal sphere are given by

$$f_{ns} = \frac{Z_{ns}}{2\pi a} u \tag{13}$$

Where: u is the *speed of sound*, a is the radius and Z_{ns} is the *acoustic Eigenvalue* of the mode. For radial modes, $n = 0$.

Figure 11 shows the Labview VI: *Calc f argon 2014.vi* that calculates f_{ns} for argon gas.

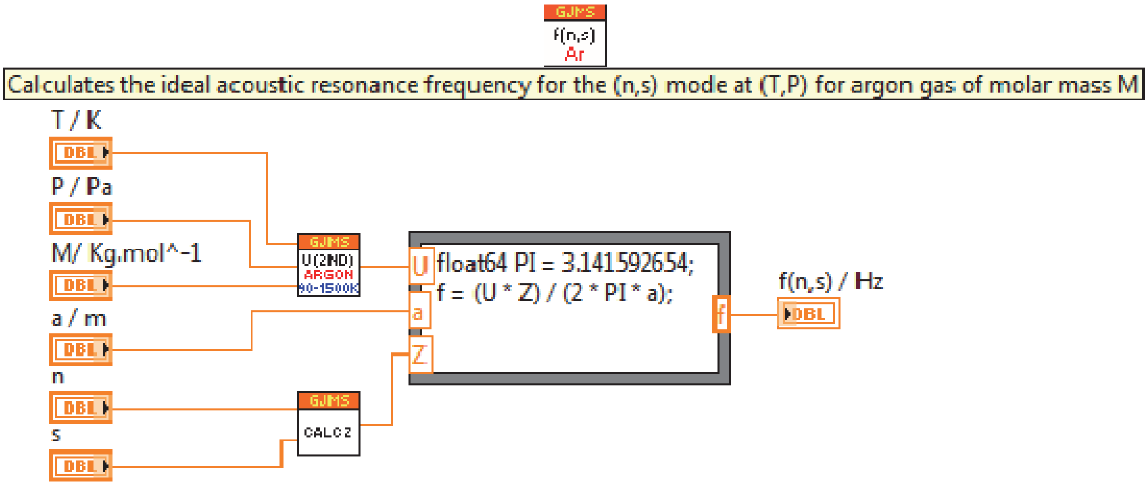

Figure 11 Labview VI: *Calc f argon 2014.vi* that calculates the acoustic Eigenvalues for a perfect sphere filled with argon gas.

13. DENSITY OF GAS: ρ [kg.m^{-3}]

The density of argon to second order in the pressure can be determined from:

$$\frac{PV}{RT} = 1 + \frac{B}{RT}P + \frac{C - B^2}{(RT)^2}P^2 \tag{14}$$

So, the molar volume is given by:

$$V = \frac{RT}{P} + B + \frac{C - B^2}{RT}P \tag{15}$$

And the mass density is then found by:

$$\rho = \frac{M}{V} \tag{16}$$

where M is the molar mass.

Figure 12 shows a plot of the mass density for various pressures and the Labview VI: *Den Argon 2014.vi* used to calculate it. Comparison with the value calculated with REFPROP [4, 5] shows excellent agreement.

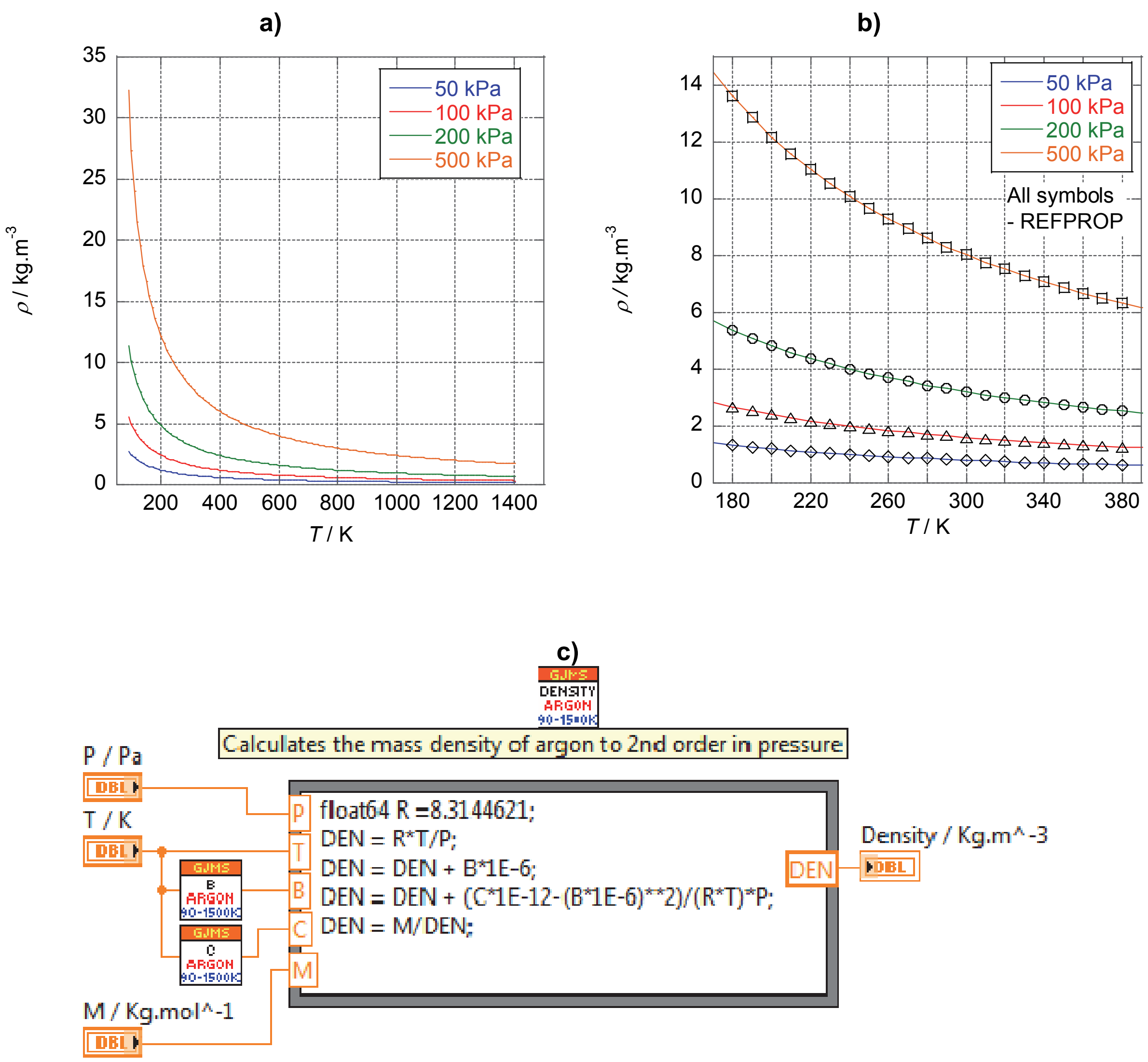

Figure 12 a) Density of argon versus T for various pressures, b) Comparison with REFPROP [3, 4] and c) The Labview VI: *Den Argon 2014.vi* used to calculate it.

14. HEAT CAPACITY AT CONSTANT PRESSURE: C_p [J.kg^{-1}.K^{-1}]

The constant pressure heat capacity is given to second order in pressure by:

$$C_p = \frac{5}{2}R - R\left[\frac{T^2}{V}\frac{\mathrm{d}^2 B}{\mathrm{d}T^2} - \frac{X}{V^2}\right] \tag{17a}$$

with

$$X = \left[\left(B - T\frac{\mathrm{d}B}{\mathrm{d}T}\right)^2 - C + T\frac{\mathrm{d}C}{\mathrm{d}T} - \frac{T^2}{2}\frac{\mathrm{d}^2 C}{\mathrm{d}T^2}\right] \tag{17b}$$

and V is the molar volume given in Equation 15.

Figure 13 shows a plot of C_p versus T for various pressures and the Labview VI: *Cp Argon 2014.vi* used to calculate it. Comparison with the value calculated with REFPROP [4, 5] shows excellent agreement.

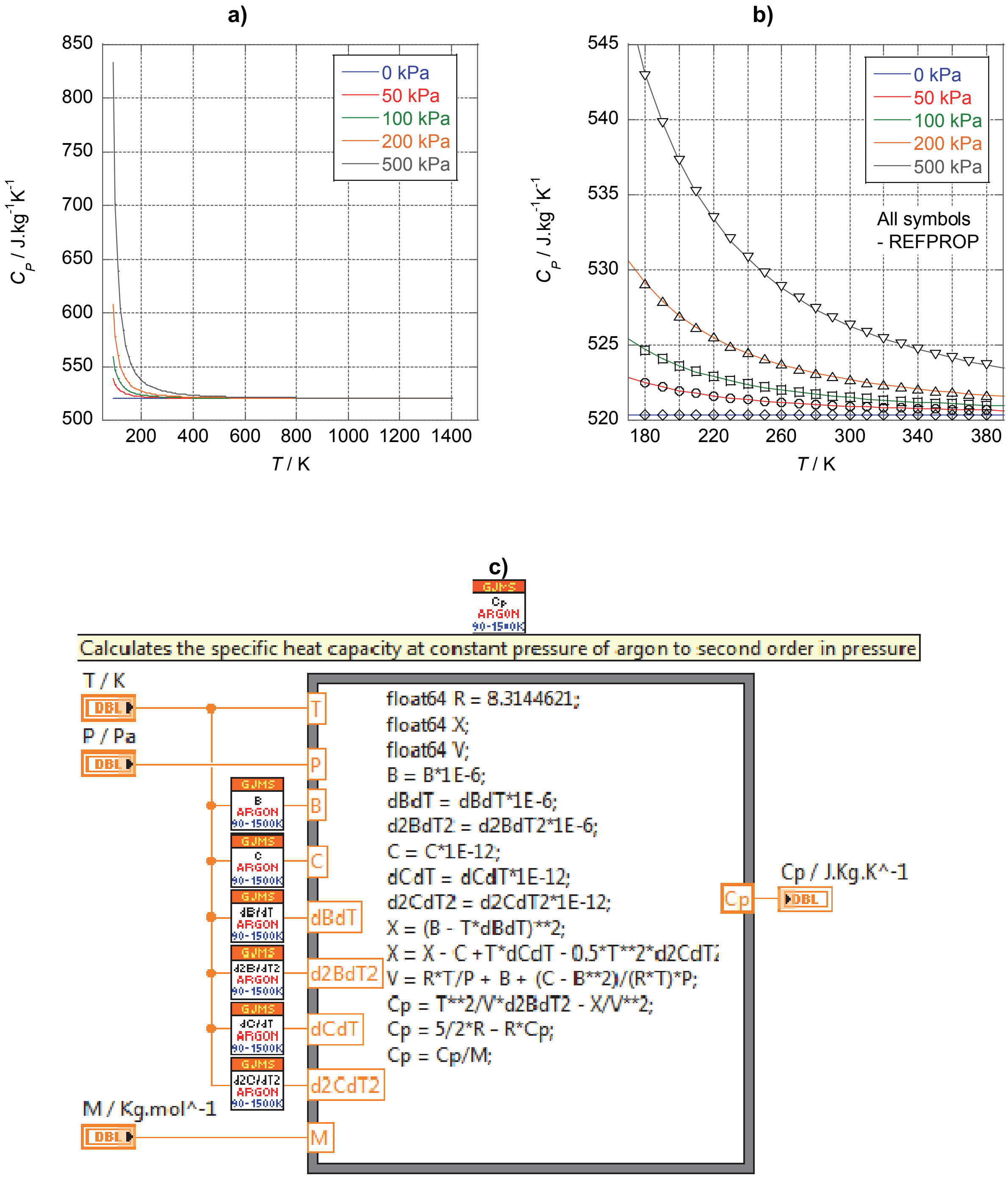

Figure 13 a) $C_P(argon)$ versus T for various pressures, b) Comparison with REFPROP [4, 5] and c) The Labview VI: *Cp Argon 2014.vi* used to calculate it.

15. HEAT CAPACITY AT CONSTANT VOLUME: C_v [J.kg^{-1}.K^{-1}]

The constant volume heat capacity is given to second order in pressure by:

$$C_V = \frac{3}{2}R - R\left[\frac{2T}{V}\frac{\mathrm{d}B}{\mathrm{d}T} + \frac{T^2}{V}\frac{\mathrm{d}^2B}{\mathrm{d}T^2} + \frac{T}{V^2}\frac{\mathrm{d}C}{\mathrm{d}T} + \frac{T^2}{2V^2}\frac{\mathrm{d}^2C}{\mathrm{d}T^2}\right] \tag{18}$$

where V is the molar volume given in Equation 15.

Figure 14 shows a plot of C_V versus T for argon at various pressures and the Labview VI: *Cv Argon 2014.vi* used to calculate it. Comparison with the value calculated with REFPROP [4, 5] shows good agreement.

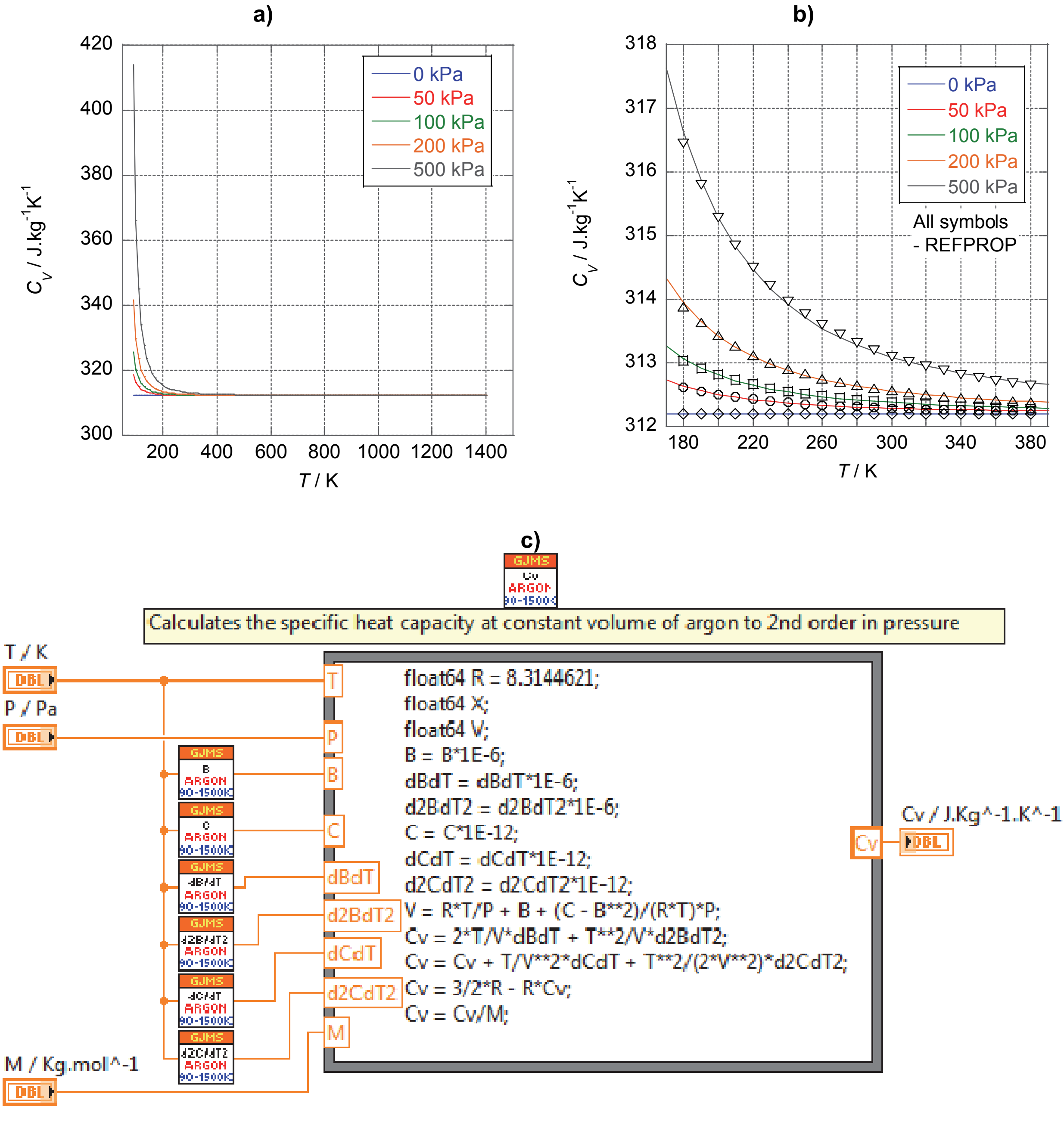

Figure 14 a) $C_V(argon)$ versus T for various pressures, b) Comparison with REFPROP [4, 5] and c) The Labview VI: *Cv Argon 2014.vi* used to calculate it.

16. RATIO OF HEAT CAPACITIES: γ

The ratio of the heat capacity at constant pressure to the heat capacity at constant volume is given by:

$$\gamma = \frac{C_P}{C_V} \tag{19}$$

Figure 15 shows a plot of this for argon at various pressures and the Labview VI: *Gamma Argon 2014.vi* used to calculate it. Comparison with the value calculated with REFPROP [4, 5] shows excellent agreement.

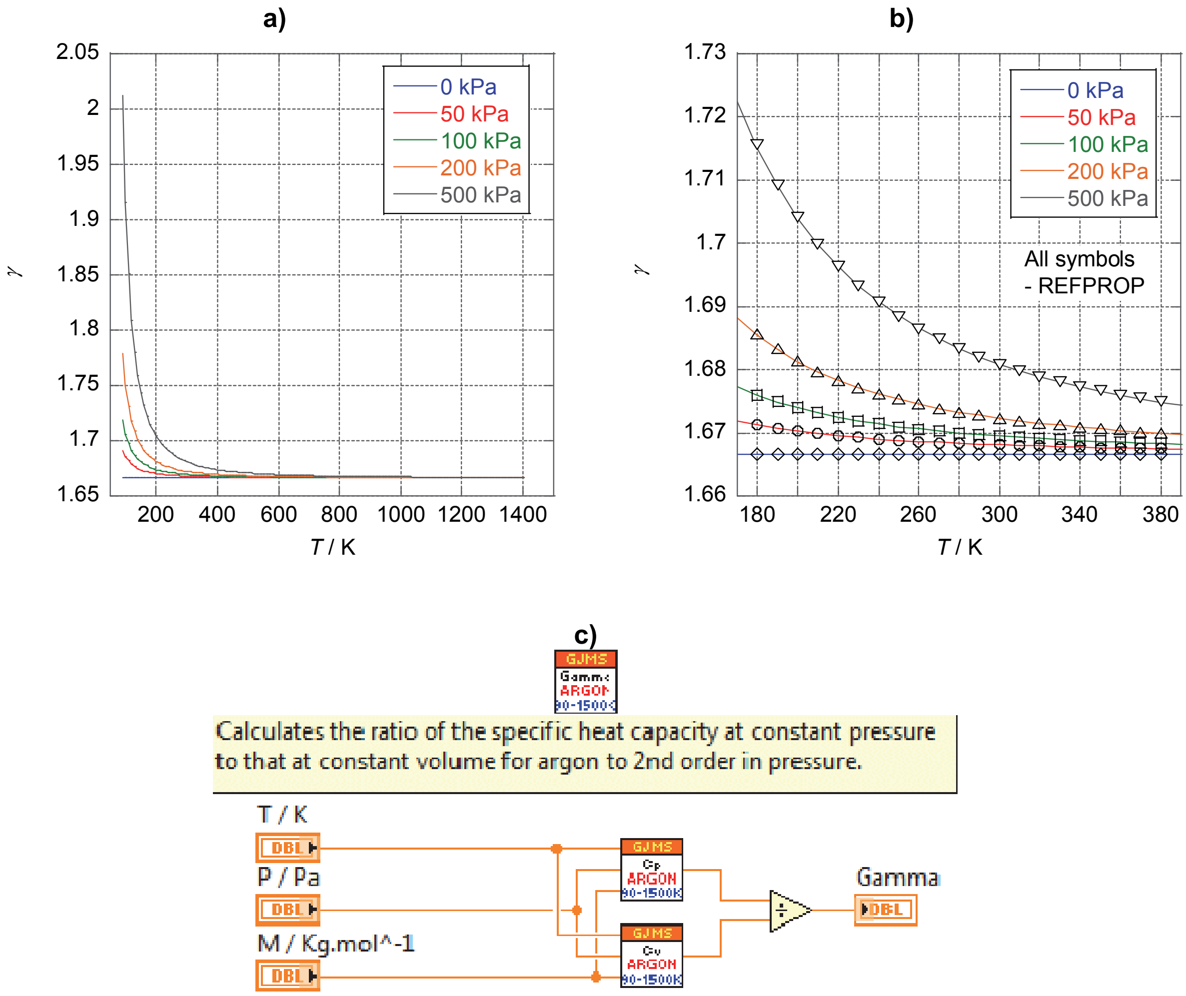

Figure 15 a) $\gamma(argon)$ versus T for various pressures, b) Comparison with REFPROP [4, 5] and c) The Labview VI: *Gamma Argon 2014.vi* used to calculate it.

17. THERMAL CONDUCTIVITY: λ [W.m^{-1}.K^{-1}]

The thermal conductivity of argon is given to second order in pressure by:

$$\lambda(T,P) = \lambda(T,0)(1 + B_\lambda(T)P + C_\lambda(T)P^2) \tag{20}$$

Where $\lambda(T,0)$ is obtained by cubic spline interpolation of the data given by *Moldover et al* [2] (reproduced in Appendix 1) and the thermal conductivity *virial* coefficients are represented by power series in T such that:

$$B_\lambda(T) = b_0 T^{b_1} \quad \text{and} \quad C_\lambda(T) = c_0 T^{c_1} \tag{21}$$

The coefficients of $B_\lambda(T)$ and $C_\lambda(T)$ are determined by fitting the pressure dependence of the thermal conductivity of argon calculated with REFPROP [4] and are shown in Table 2. In determining these coefficients, the pressure units were in kPa.

Coefficient	Value
b_0	0.239835
b_1	-1.659458
c_0	8918.5
c_1	-5.40261

Table 2 Thermal conductivity *virial* coefficients for argon.

Figure 16 a) shows the thermal conductivity of argon versus T for pressures from 0 kPa to 1000 kPa, with parts b) and c) showing the small pressure dependent component with *least squares* fits and part d) showing the fitting residuals. The Labview VI: *Therm cond argon 2014.vi* used to calculate it is shown in Figure 16 e).

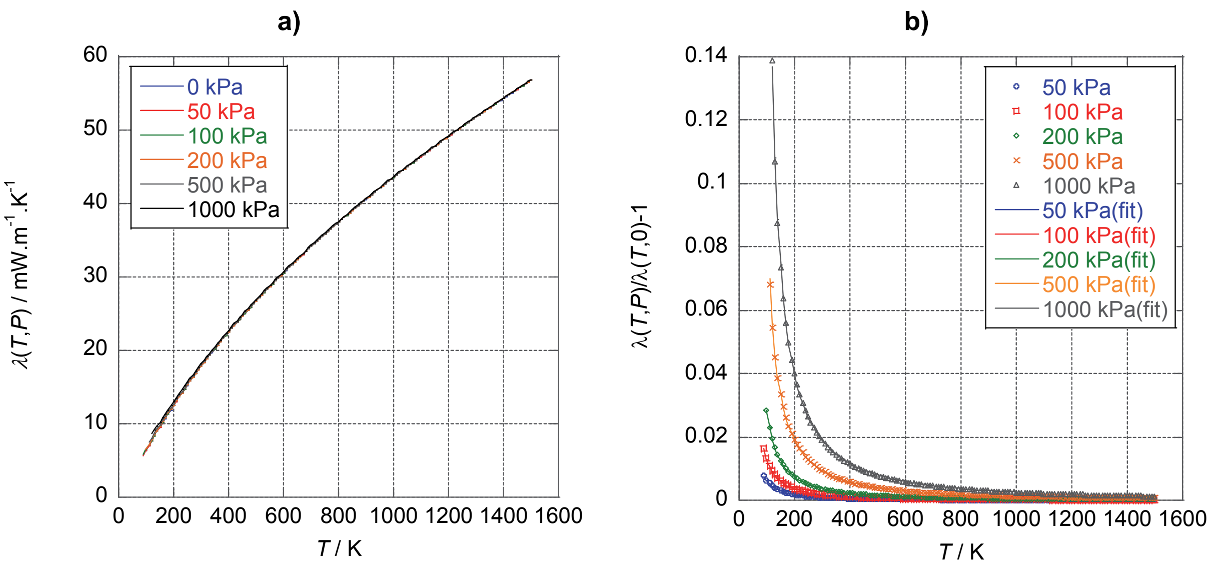

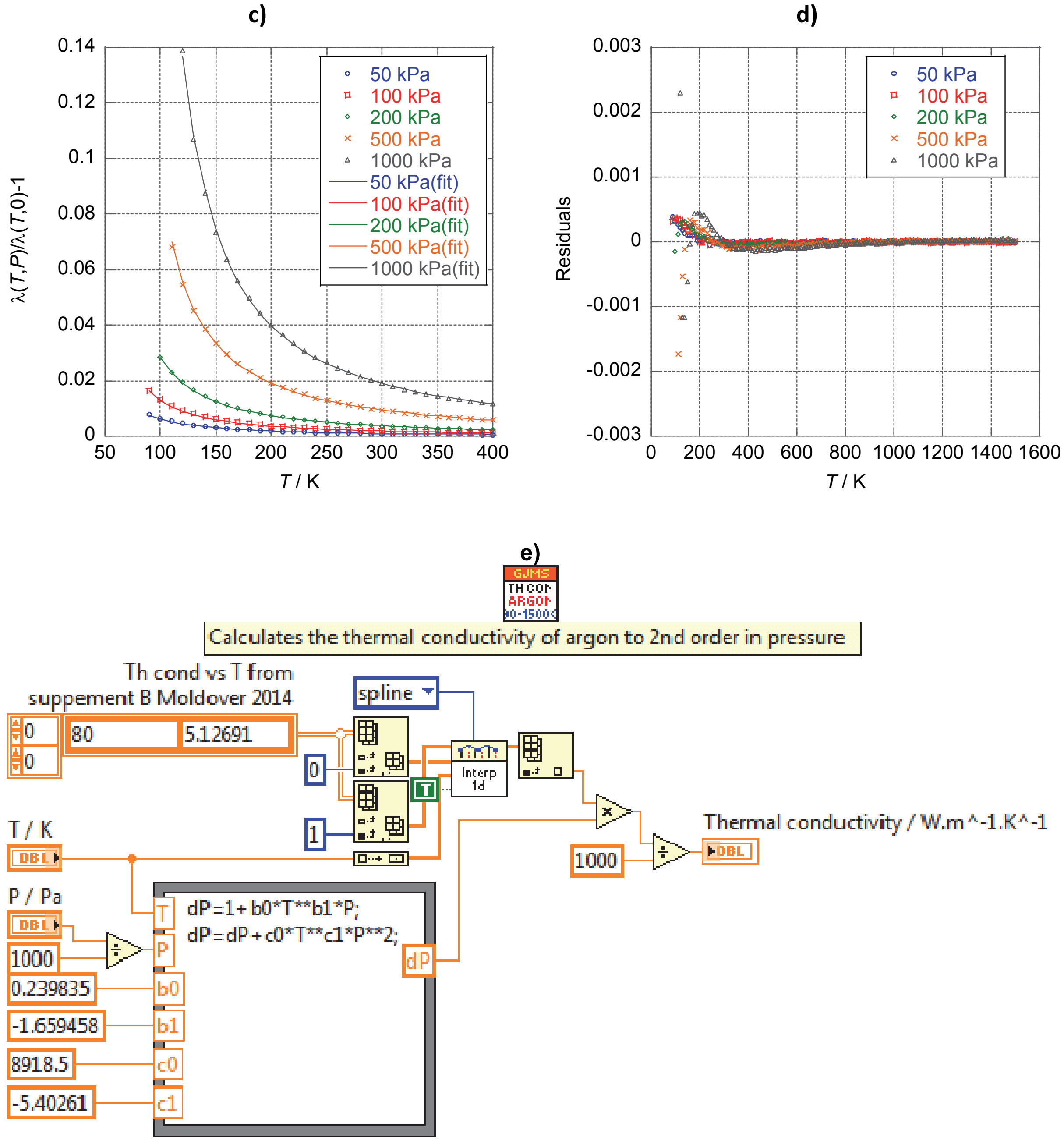

Figure 16 a) Thermal conductivity of argon versus T for pressures from 0 kPa to 1000 kPa, b) & c) the small pressure dependent component with fits, d) the fitting residuals and e) the Labview VI: *Therm cond argon 2014.vi* used to calculate it.

18. VISCOSITY: η [Pa.s]

The viscosity of argon is given to second order in pressure by:

$$\eta(T,P) = \eta(T,0)\left(1 + B_\eta(T)P + C_\eta(T)P^2\right) \tag{22}$$

Where, $\eta(T,0)$ is obtained by cubic spline interpolation of the data given by *Moldover et al* [1] (reproduced in Appendix 1) and the viscosity *virial* coefficients are represented by power series in T such that:

$$B_\eta(T) = b_0 T^{b_1} \qquad \text{and} \qquad C_\eta(T) = c_0 T^{c_1} \tag{23}$$

The coefficients of $B_\eta(T)$ and $C_\eta(T)$ are determined by fitting the pressure dependence of the viscosity of argon calculated with REFPROP [4] and are shown in Table 3. In determining these coefficients, the pressure units were in kPa.

Coefficient	Value
b_0	0.285393
b_1	-1.843401
c_0	9984.41
c_1	-5.73185

Table 3 Viscosity *virial* coefficients for argon.

Figure 17 a) shows the viscosity of argon versus T for pressures from 0 kPa to 1000 kPa, with parts b) and c) showing the small pressure dependent component with *least squares* fits and d) showing the fitting residuals. The Labview VI: *Visc argon 2014.vi* used to calculate it is shown in Figure 16 e).

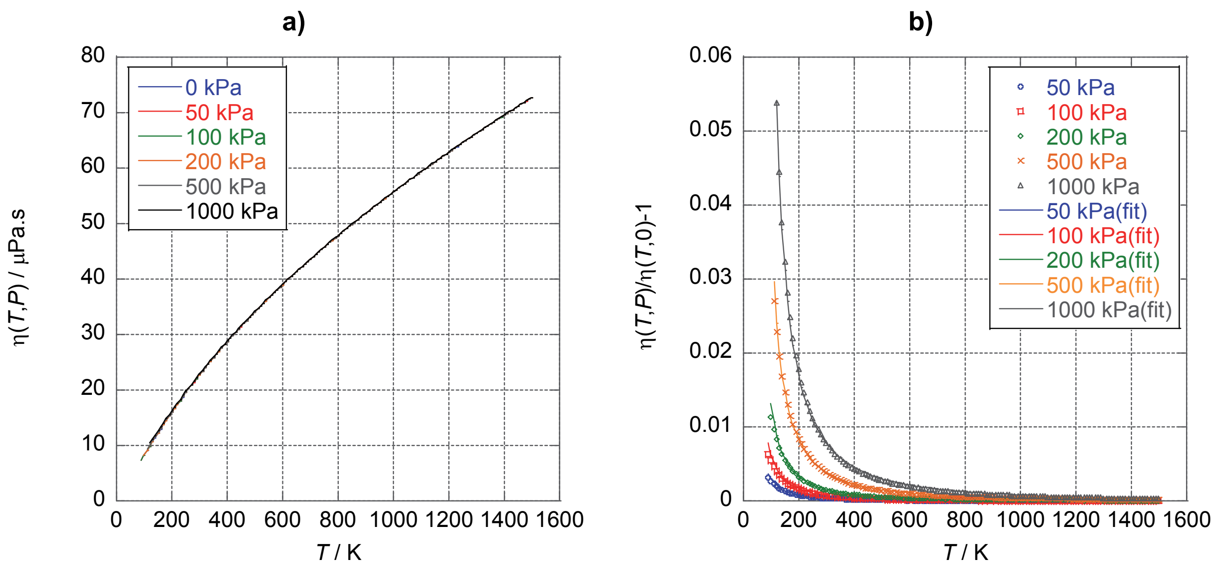

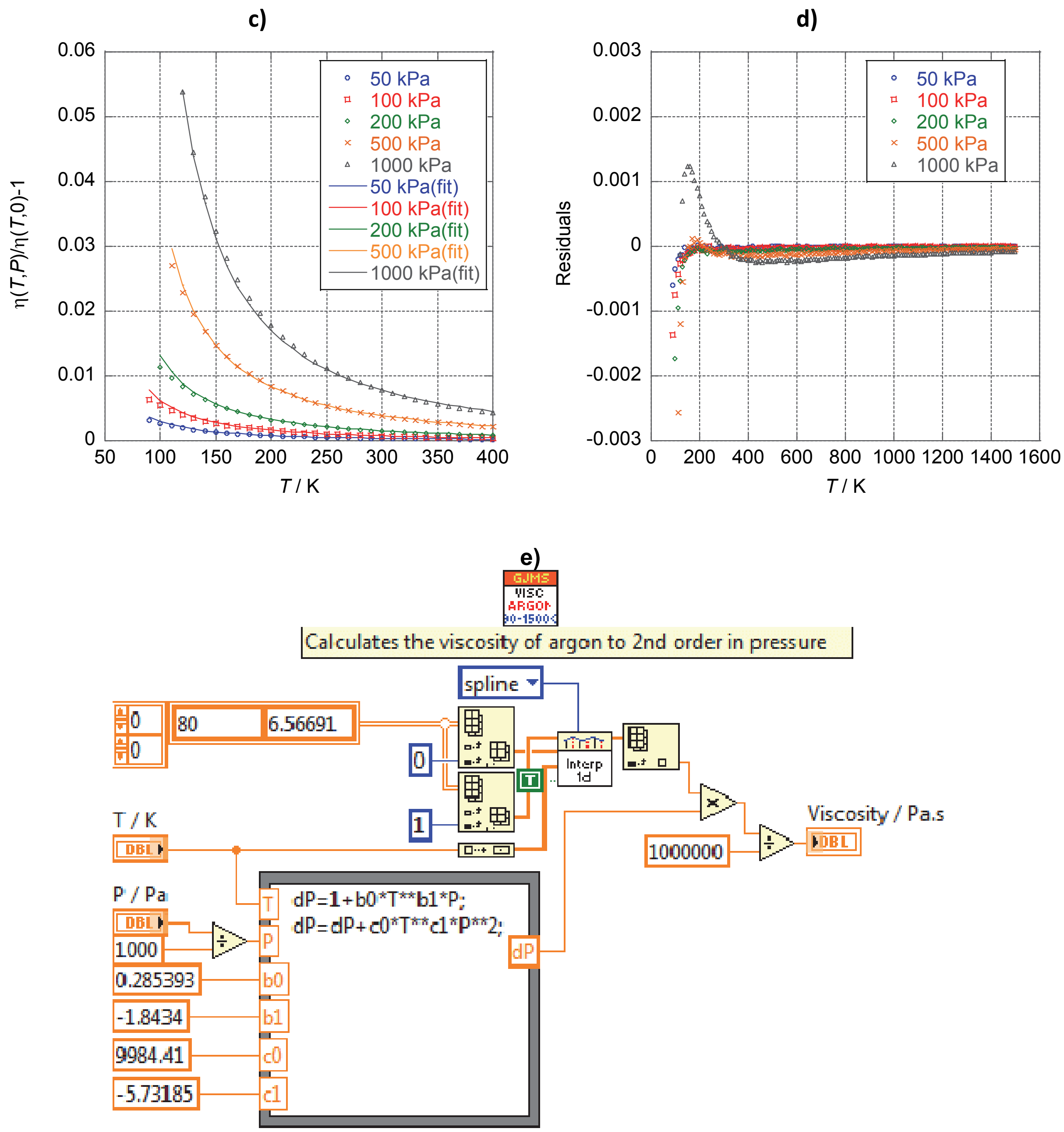

Figure 17 a) Viscosity of argon versus T for pressures from 0 kPa to 1000 kPa, b) & c) the small pressure dependent component with fits, d) the fitting residuals and e) the Labview VI: *Visc argon 2014.vi* used to calculate it.

19. THERMAL PENETRATION LENGTH: δ_{th} [m]

The *thermal penetration length* is given by:

$$\delta_{th} = \left(\frac{\lambda}{\pi\rho C_P f}\right)^{0.5} \tag{24}$$

Where:

λ is the thermal conductivity.
ρ is the density.
C_P is the specific heat capacity at constant pressure.
f is the acoustic frequency.

Figure 18 shows the thermal penetration length for the (0,2) mode of an argon filled sphere of 62 mm radius and the Labview VI: *Th pen argon 2014.vi* used to calculate it.

a)

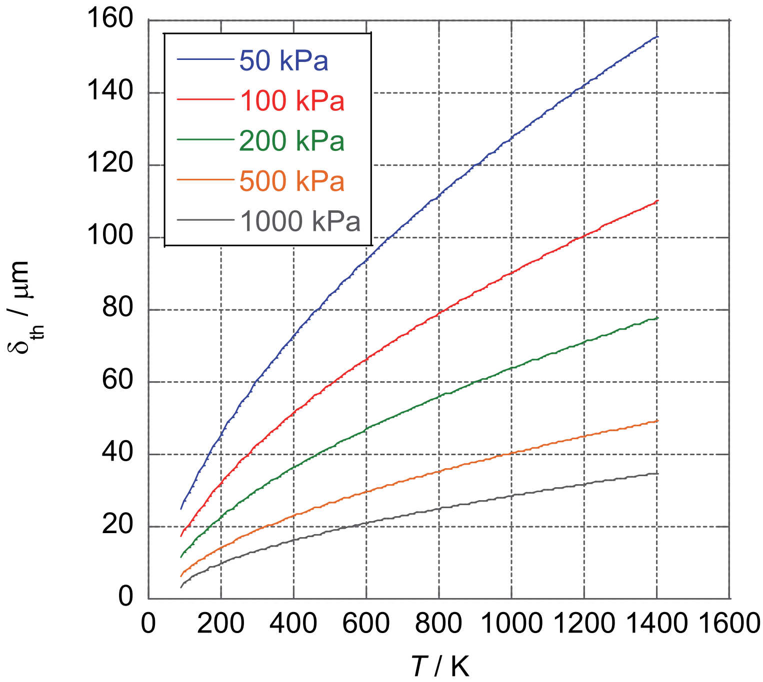

b)

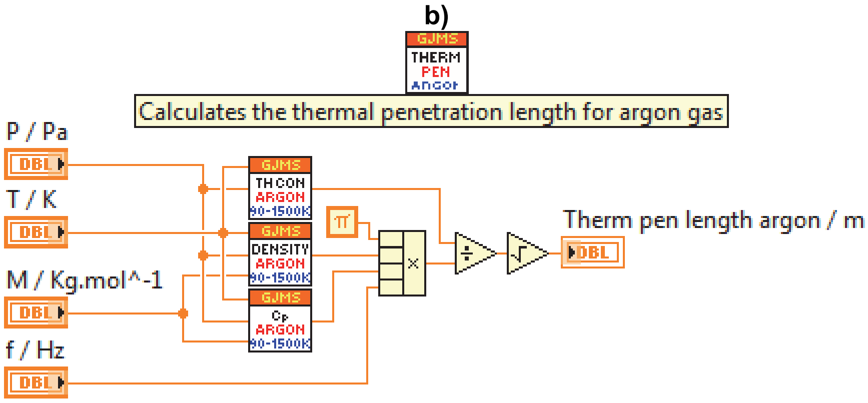

Figure 18 a) The *thermal penetration length* for the (0,2) mode of an argon filled sphere of 62 mm radius and b) the Labview VI: *Th pen argon 2014.vi* used to calculate it.

20. VISCOUS PENETRATION LENGTH: δ_v [m]

The *viscous penetration length* is given by:

$$\delta_v = \left(\frac{\eta}{\pi\rho f}\right)^{0.5} \tag{25}$$

Where:

η is the viscosity.
ρ is the density.
f is the acoustic frequency.

Figure 19 shows the *viscous penetration length* for the (0,2) mode of an argon filled sphere of 62 mm radius and the Labview VI: *Visc pen argon 2014.vi* used to calculate it.

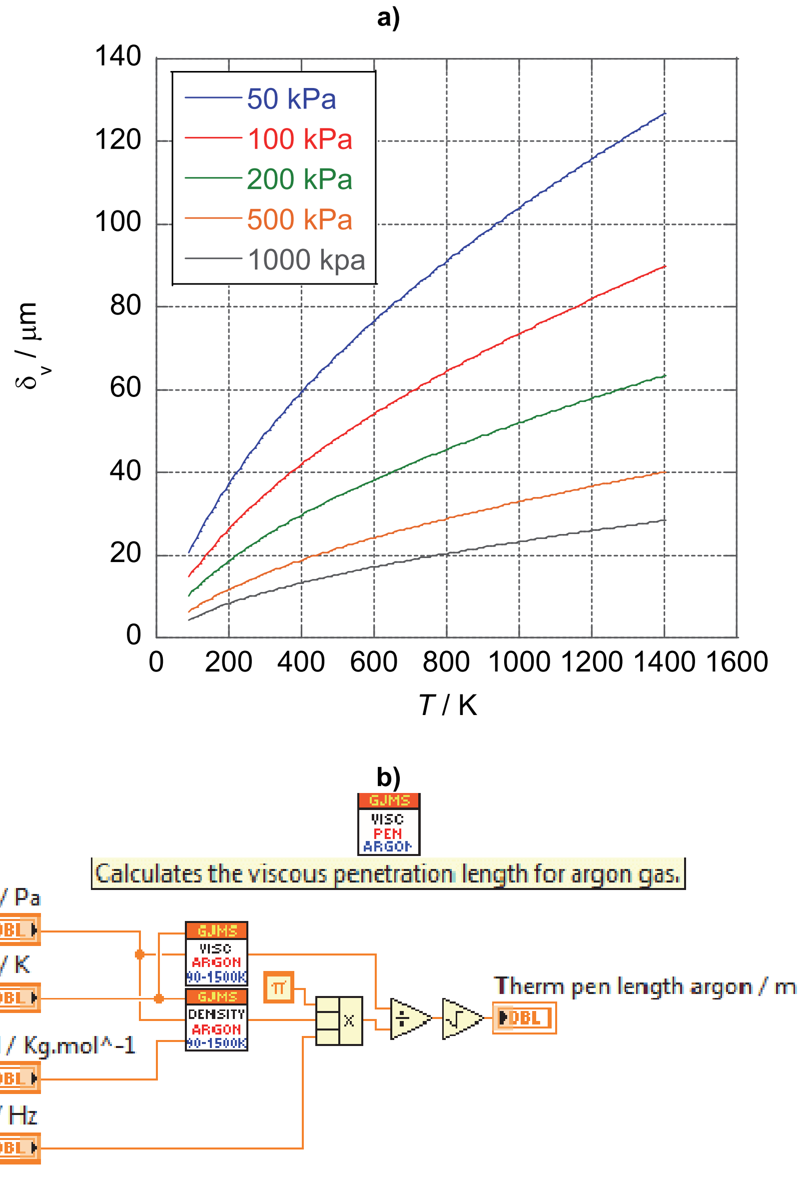

Figure 19 a) The *viscous penetration length* for the (0,2) mode of an argon filled sphere of 62 mm radius and b) the Labview VI: *Visc pen argon 2014.vi* used to calculate it.

21. THERMAL ACCOMMODATION LENGTH: l_{th} [m]

The *thermal accommodation length* of a gas is given by:

$$l_{th} = \frac{\lambda}{P}\left(\frac{\pi M T}{2R}\right)^{0.5}\left(\frac{2-h}{h}\right)\left(\frac{1}{C_V M/R + 1/2}\right) \tag{26}$$

Where h is the *thermal accommodation coefficient* that depends on the gas and surface of the sphere (material, surface finish) and must be found experimentally.

Figure 20 shows the *thermal accommodation length* for h = 0.85 for argon gas and the Labview VI: *Th acc argon 2014.vi* used to calculate it.

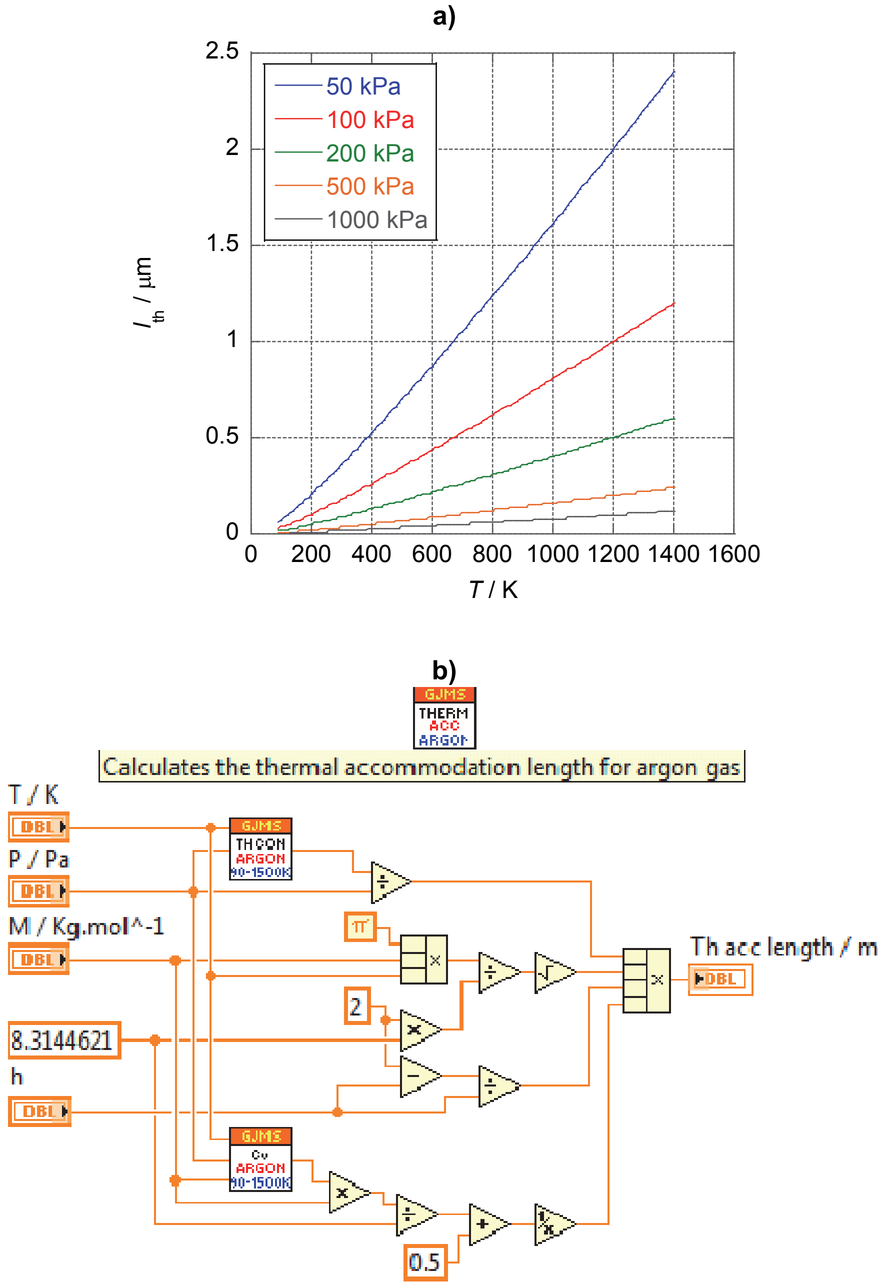

Figure 20 a) The *thermal accommodation length* for h = 0.85 for argon gas and b) the Labview VI: *Th acc argon 2014.vi* used to calculate it.

22. THERMAL CONDUCTIVITY OF COPPER: λ_{Cu} [W.m^{-1}.K^{-1}]

The thermal conductivity of copper over the temperature range 90 K – 1350 K can be determined by cubic spline interpolation of the data provided by NIST [6]. Figure 21 shows this data, the fit and the Labview VI: *Therm cond Cu 2014.vi* that is used to calculate it.

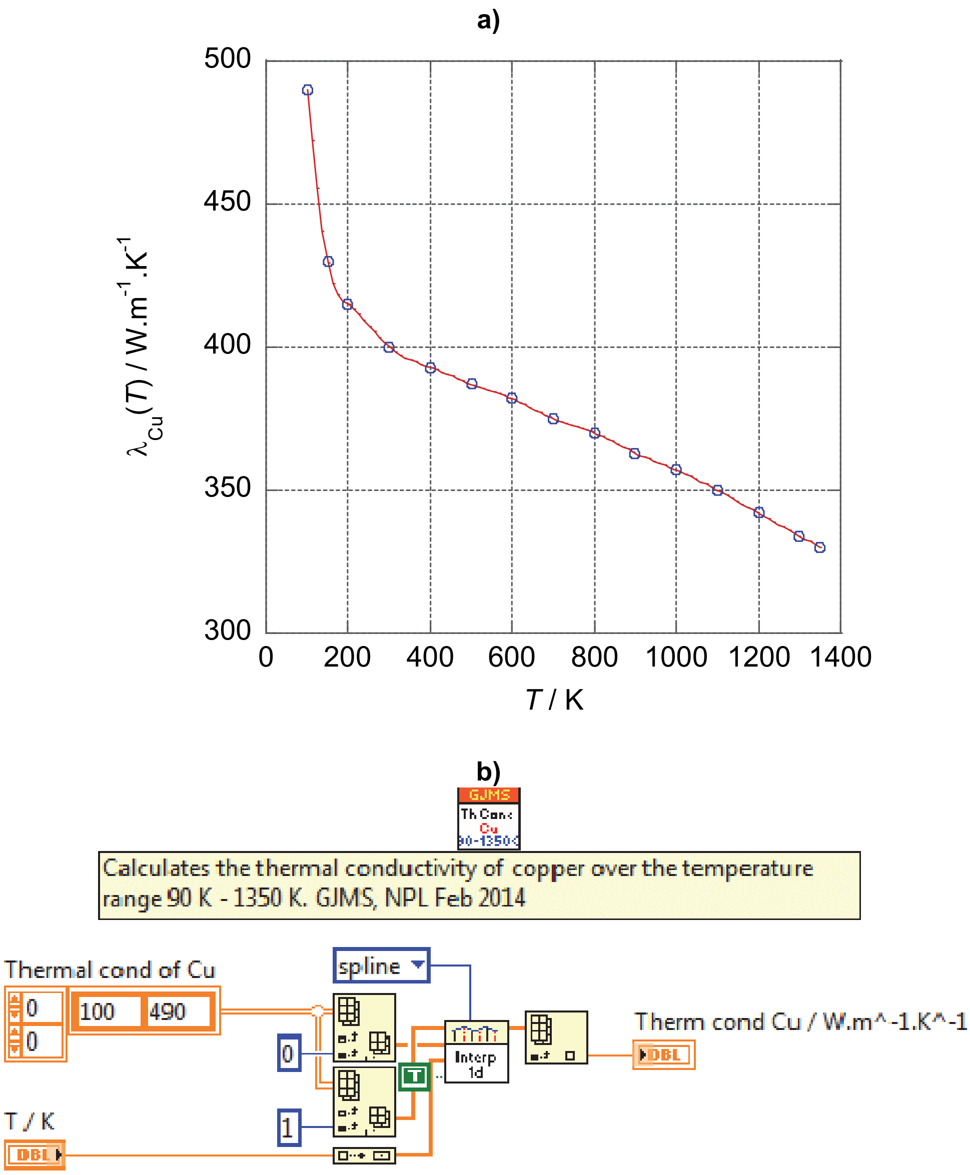

Figure 21 a) The *thermal conductivity* of copper and b) the Labview VI: *Therm cond Cu 2014.vi* used to calculate it.

23. HEAT CAPACITY OF COPPER: $C_{p,Cu}$ [J.kg^{-1}.K^{-1}]

The *specific heat capacity* of copper over the temperature range 90 K – 1350 K can be determined by cubic spline interpolation of the data provided by *White et al* [7]. Figure 22 shows this data, the fit and the Labview VI: *Cp Cu 2014.vi* that is used to calculate it.

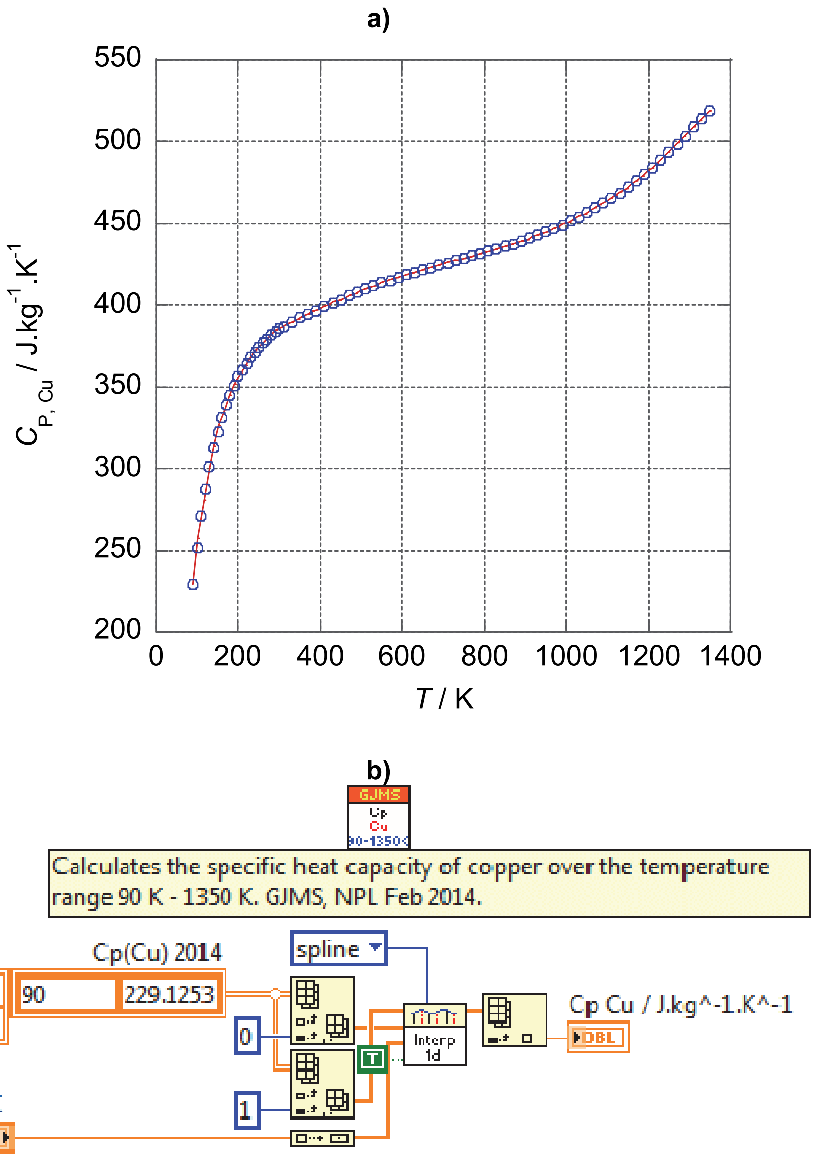

Figure 22 a) The *specific heat capacity* of copper and b) the Labview VI: *Cp Cu 2014.vi* used to calculate it.

24. THERMAL PENETRATION LENGTH FOR COPPER: $\delta_{th,Cu}$ [m]

The *thermal penetration length* for copper is given by:

$$\delta_{th,Cu} = \left(\frac{\lambda_{Cu}}{\pi \rho_{Cu} C_{P,Cu} f}\right)^{0.5} \tag{27}$$

Figure 23) shows the *thermal penetration length* for copper for the first 5 radial modes of an argon filled sphere of radius 0.062 m at 100 kPa. The Labview VI: *Th pen Cu 2014.vi* used to calculate it is also shown.

a)

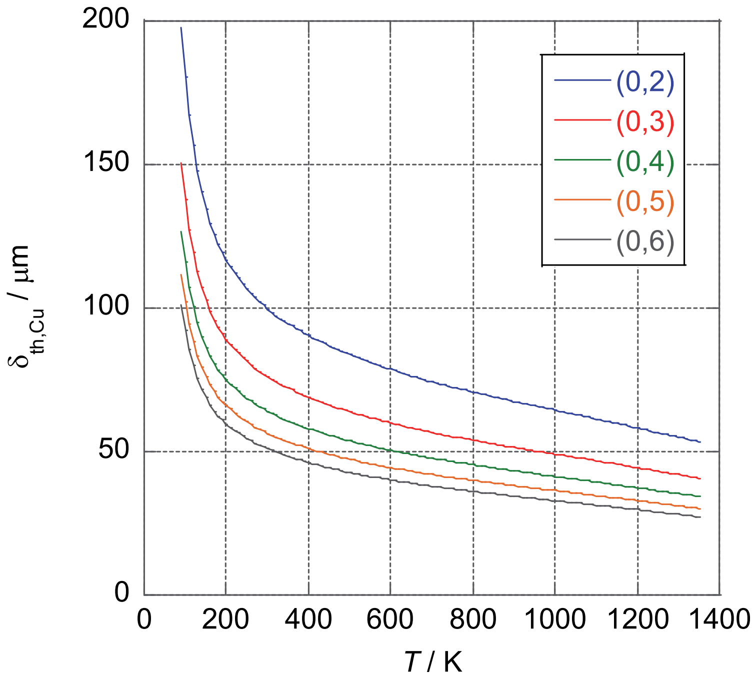

b)

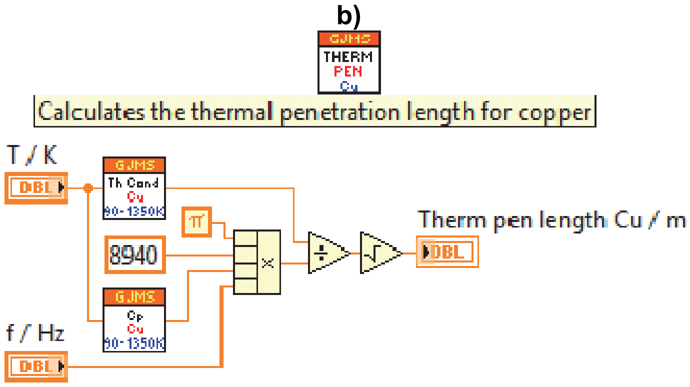

Figure 23 a) The *thermal penetration length* for copper for the first 5 radial modes of an argon filled sphere of radius 0.062 m at 100 kPa and b) the Labview VI: *Th pen Cu 2014.vi* used to calculate it.

25. THERMAL BOUNDARY LAYER PERTURBATION: $(\Delta f/f_0)_{TBL}$, $(g/f_0)_{TBL}$

The *thermal boundary layer* perturbation to the radial acoustic modes combines the *thermal penetration length* δ_{th}, the *thermal accommodation length* l_{th}, and the *thermal penetration length* of the shell (assumed to be copper) $\delta_{th,Cu}$. It can be written in terms of the fractional shift in resonance frequency from the ideal frequency $(\Delta f/f_0)_{TBL}$ and the fractional contribution to the resonance half-width $(g/f_0)_{TBL}$ [2] as:

$$\left(\frac{\Delta f}{f_0}\right)_{TBL} = -\frac{(\gamma-1)}{2a}\delta_{th} + \frac{(\gamma-1)}{a}l_{th} + \frac{(\gamma-1)}{2a}\delta_{th,Cu}\frac{\lambda_{gas}}{\lambda_{Cu}} \tag{28a}$$

$$\left(\frac{g}{f_0}\right)_{TBL} = \frac{(\gamma-1)}{2a}\delta_{th} + \frac{(\gamma-1)}{2a}\delta_{th,Cu}\frac{\lambda_{gas}}{\lambda_{Cu}} - \frac{1}{2}(\gamma-1)(2\gamma-1)\left(\frac{\delta_{th}}{a}\right)^2 \tag{28b}$$

Where:

f_0 is the ideal resonance frequency.
λ_{gas} is the *thermal conductivity* of the gas.
λ_{Cu} is the thermal *conductivity* of the shell (copper).
a is the average radius of the sphere.
δ_{th} is the *thermal penetration length* of the gas (argon).
$\delta_{th,Cu}$ is the *thermal penetration length* of the shell (copper).
l_{th} is the *thermal accommodation length* of the gas/shell.

The last term on the RHS of Equation 28b is the second order correction of *Gillis* [8] and only applies to the half-width.

Figure 24 shows the TBL perturbation to the (0,2) radial acoustic mode for an argon-filled copper sphere of radius 0.062 m versus pressure, for temperatures from 100 K to 1400 K. The thermal accommodation coefficient is assumed to be $h = 0.85$. The Labview VI: *TBL argon 2014.vi* that calculates it is also shown.

It should be noted that the VI calculates and outputs $(\Delta f/f_0)_{TBL}$, $(g/f_0)_{TBL}$ and an estimate of the ideal resonance frequency $\langle f_0 \rangle$ based on the input parameters. The corrected frequency and the TBL contribution to the half-width are therefore given by:

$$f_0 = f_{meas} - \left(\frac{\Delta f}{f_0}\right)_{TBL}\langle f_0 \rangle \tag{29a}$$

$$g = \left(\frac{g}{f_0}\right)_{TBL}\langle f_0 \rangle \tag{29b}$$

Where f_{meas} is the measured resonance frequency. Since $(\Delta f/f_0)_{TBL}$ is negative, $f_0 > f_{meas}$.

Note: the difference between $(\Delta f/f_0)f_0$ and $(\Delta f/f_0)f_{meas}$ is of order $(\Delta f/f_0)^2$ which may be significant in some situations.

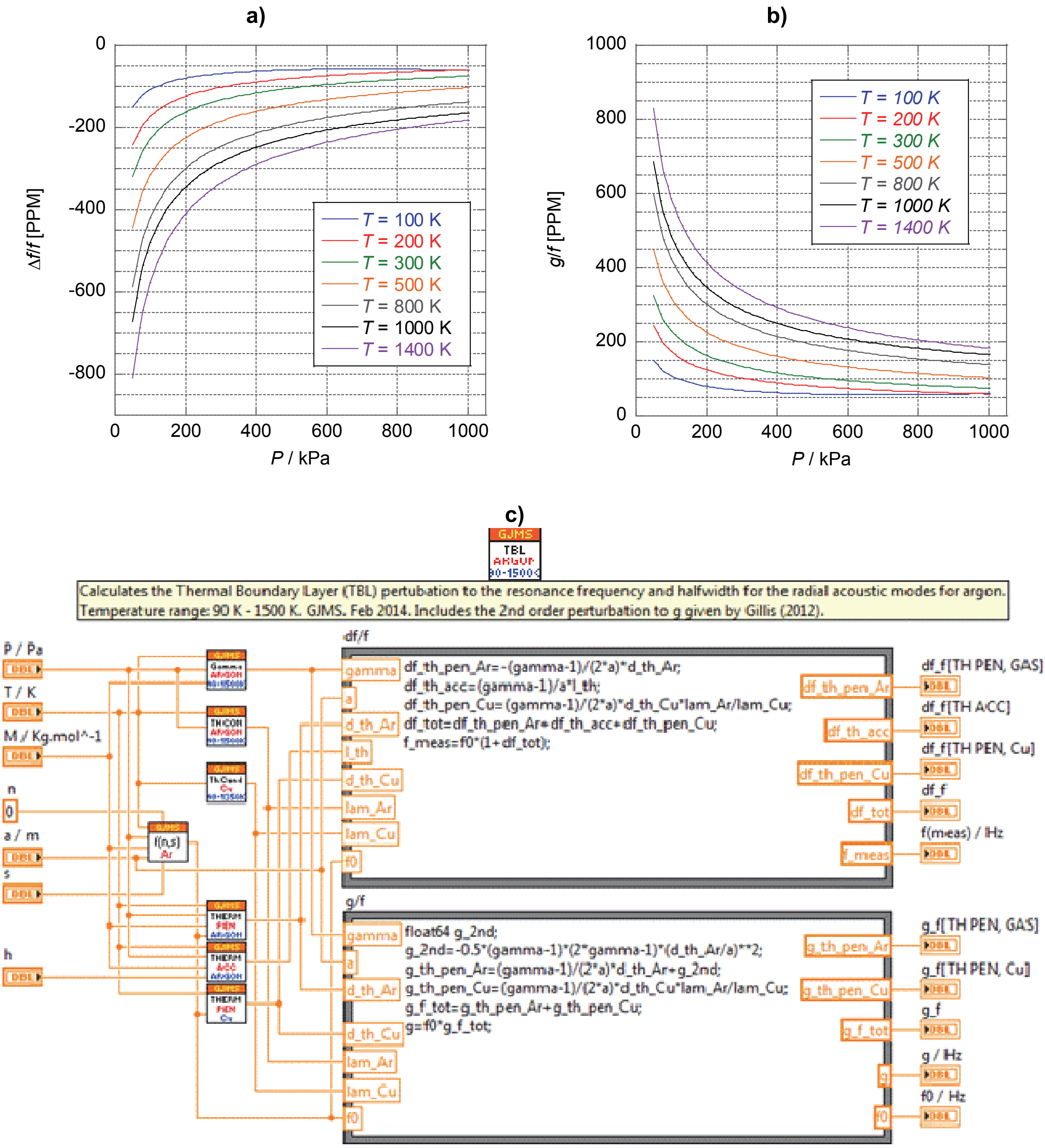

Figure 24 The *thermal boundary layer* perturbation for argon gas in a spherical acoustic resonator of 62 mm radius for the (0,2) radial acoustic mode: a) $(\Delta f/f_0)_{TBL}$ and b) $(g/f_0)_{TBL}$ and c) the Labview VI: *TBL argon 2014.vi* that calculates it.

26. BULK DISSIPATION: $(g/f_0)_{bulk}$

The bulk dissipation perturbation takes into account the dissipation of the acoustic energy in the bulk of the gas itself. This is observed as an additional contribution to the resonance half-width g and is given by:

$$\left(\frac{g}{f_0}\right)_{bulk} = f_0^2 \frac{\pi^2}{u^2}\left[\frac{4}{3}\delta_v^2 + (\gamma - 1)\delta_{th}^2\right] \tag{30}$$

Where:

δ_v is the *viscous penetration length*.
δ_{th} is the *thermal penetration length*.
u is the speed of sound.

Figure 25 shows the *bulk dissipation perturbation* for the (0,2) radial acoustic mode of an argon-filled sphere of 62 mm radius, $(g/f_0)_{bulk}$ and the Labview VI: *Bulk dis argon 2014.vi* that calculates it.

a)

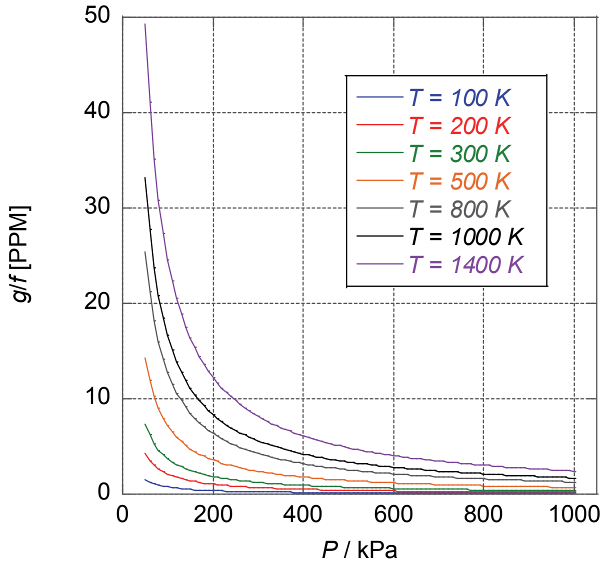

b)

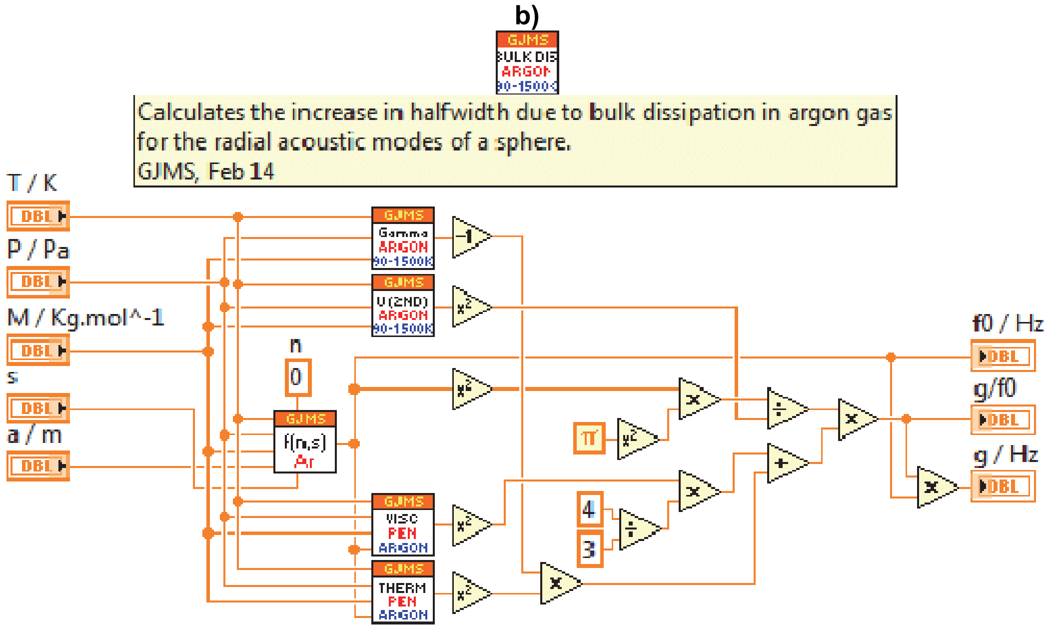

Figure 25 The *bulk dissipation perturbation* for argon: a) the perturbation to the (0,2) radial acoustic mode for a sphere of 62 mm radius, $(g/f_0)_{bulk}$ and b) the Labview VI: *Bulk dis argon 2014.vi* that calculates it.

27. SPEED OF SOUND IN COPPER: $u_{L,Cu}$ [m.s^{-1}]

The longitudinal speed of sound in copper is given by [5]:

$$u_{L,Cu} = \left[\frac{(1-\sigma)}{(1-2\sigma)(1+\sigma)}\frac{E_{Cu}}{\rho_{Cu}}\right]^{0.5} \tag{31}$$

Where:

σ is *Poisson's ratio*, equal to 0.343 for copper.
E_{Cu} is *Young's modulus*, equal to 129.8 GPa for copper.
ρ_{Cu} is the *density*, equal to 8940 kg.m^{-3} for copper.

For these parameters, $U_{L,Cu}$ = 4758 m.s^{-1}. Figure 26 shows the Labview VI: *U long Cu 2014.vi* that calculates it.

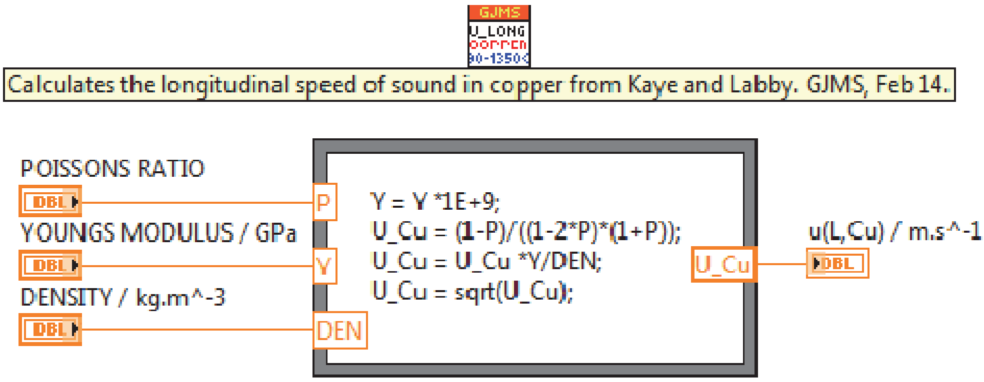

Figure 26 The Labview VI: : *U long Cu 2014.vi* used to calculate the longitudinal speed of sound in copper.

28. TRANSDUCER PERTURBATION: $(\Delta f/f)_{tr}$

The perturbation to a radial acoustic mode in a spherical cavity induced by the presence of a microphone can be calculated with:

$$\left(\frac{\Delta f}{f_0}\right)_{tr} = -\frac{\rho u^2}{2}\frac{r_{tr}^2}{a^3}X_{tr} \tag{32}$$

Where:

ρ is the gas density.
u is the speed of sound.
r_{tr} is the radius of the microphone membrane.
a is the radius of the sphere.
X_{tr} is the compliance per unit area of the microphone membrane.

This perturbation must be subtracted from the measured frequency to obtain the ideal frequency and for a typical arrangement with two similar microphones (one used as a speaker), must be doubled.

Figure 27 shows a) the typical parameters for a Brüel and Kjaer ¼ inch microphone, b) the perturbation to the (0,2) radial acoustic mode of an argon filled sphere of 62 mm radius due to a single ¼ inch microphone (at $T = 273.16$ K – although the product ρu^2 is almost independent of T as is the perturbation) and c) the Labview VI used to calculate it: *Trans pert argon 2014.vi*.

a)

Parameter	
T / K	273.16
a / mm	50.00
r_{tr} / mm	2.50
X_m / mPa^{-1}	1.5E-10

b)

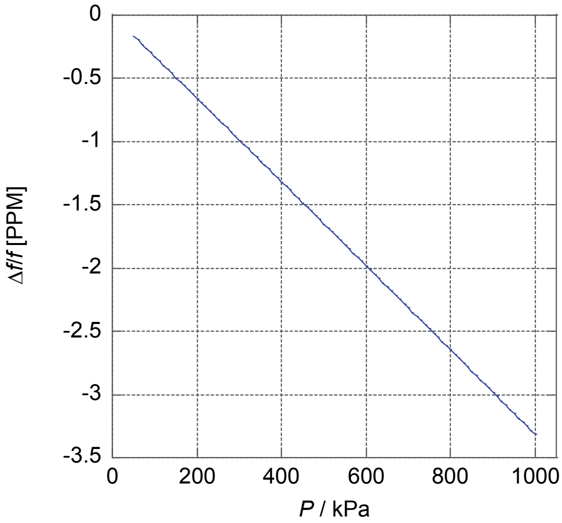

c)

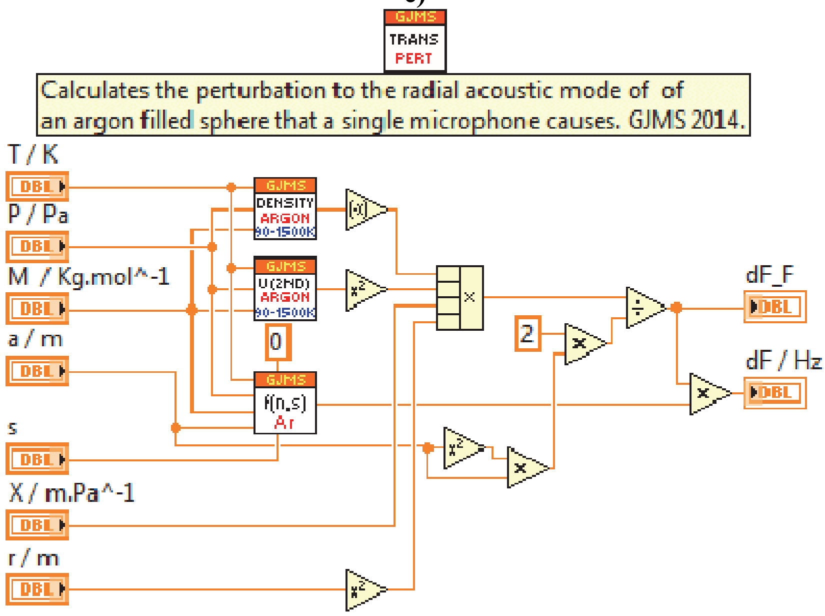

Figure 27 The acoustic transducer perturbation: a) typical parameters for a B&K ¼” microphone, b) the perturbation to the (0,2) radial acoustic mode of an argon filled sphere of 62 mm radius due to a single ¼” microphone (at T = 273.16 K) and c) the Labview VI used to calculate it: *Trans pert argon 2014.vi*.

29. DETERMINATION OF THE SPEED OF SOUND SQUARED: $u_m(T,P)$ [m^2.s^{-2}]

Once, the measured resonance frequency of the radial acoustic mode has been corrected for all perturbations, the speed of sound squared can be calculated with:

$$u_m^2(T,P) = \left(\frac{2\pi f_{0s}}{Z_{0s}}\right)^2 a^2(T,P) \tag{33}$$

where Z_{0s} is the eigenvalue of the s^{th} radial mode.

30. THE SECOND-ORDER SHAPE PERTURBATION FOR A TRIAXIAL ELIPSOID: ($\Delta Z_{0s}^2/Z_{0s}^2$)

The second-order shape perturbation [9], which accounts for the fact that the sphere is a triaxial ellipsoid, can be calculated using:

$$\frac{\Delta Z_{0s}^2}{Z_{0s}^2} = \frac{8Z_{0s}^2}{135}(\varepsilon_1^2 - \varepsilon_1\varepsilon_2 + \varepsilon_2^2) \tag{34}$$

where Z_{0s} is the eigenvalue of the s^{th} radial mode and ε_1 and ε_2 are the eccentricities of the sphere calculated from microwave measurements. This is effectively a correction on u^2, not f and should be subtracted from the measurement as:

$$u_{s,corr}^2 = u_s^2\left(1 - \frac{\Delta Z_{0s}^2}{Z_{0s}^2}\right) \tag{35}$$

Figure 28 shows the second-order shape perturbation for a quasi-sphere with ε_1 = 0.001 and ε_2 = 0.0005 and the Labview VI used to calculate it: *2nd order shape pert 2014.vi*.

a)

	ε_1	**0.001**
	ε_2	**0.0005**
s	Z_{0s}	$\Delta Z_{0s}^2/Z_{0s}^2$ **[PPM]**
2	4.49341	0.897
3	7.72525	2.652
4	10.9041	5.284
5	14.0662	8.794
6	17.2208	13.18
7	20.3713	18.444
8	23.5195	24.585
9	26.6661	31.603
10	29.8116	39.499

b)

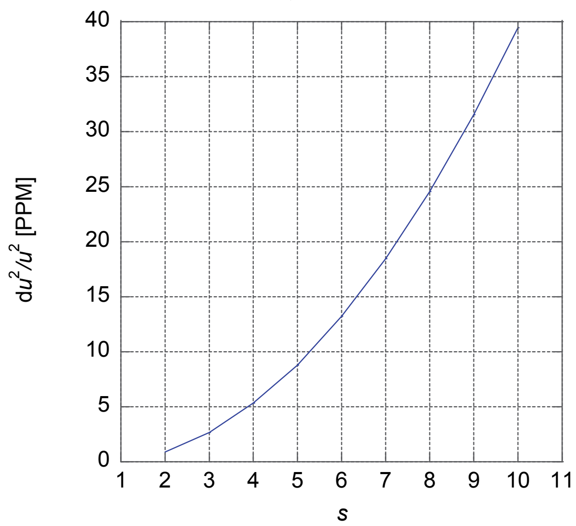

c)

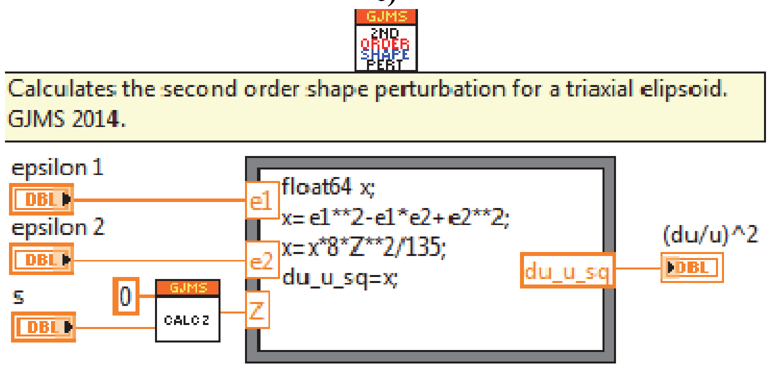

Figure 28 The second order shape perturbation for a sphere with ε_1 = 0.001 and ε_2 = 0.0005: a) tabulated data, b) plotted data, and c) the Labview VI used to calculate it: *2nd order shape pert 2014.vi*.

31. THE *SPEED OF SOUND SQUARED* CORRECTED TO T_1 : $u_m^2(T_1, P)$ [m^2.s^{-2}]

Measurements of the *speed of sound squared* made at T_0 (close to T_1) may need correcting to that at T_1. This can be achieved by:

$$u_m^2(T_1, P) = u_m^2(T_0, P)\frac{T_1}{T_0}\frac{\left(1 + \frac{\beta(T_1)}{RT_1}P\right)}{\left(1 + \frac{\beta(T_0)}{RT_0}P\right)} \tag{36}$$

Where β is the 2nd *acoustic virial coefficient* and R is the molar gas constant.

32. EXPERIMANTAL DETERMINATION OF THE SHELL BREATHING MODE FREQUENCY AND SECOND ACOUSTIC VIRIAL COEFFICIENT: f_{breath} [Hz], β [cm^3.mol^{-1}]

The measured resonance frequencies are perturbed by coupling to the breathing mode of the resonator. For a given isotherm, this perturbation is mode-dependent and approximately linearly proportional to the pressure. If all the data is to be fitted together, this can be accounted for by fitting a different A_{1s} coefficient for each radial mode $(0, s)$:

$$u^2(T, P) = A_0(1 + A_{1s}P + A_2P^2 + \cdots) \tag{37}$$

When this has been done, the breathing mode perturbation is clearly visible when A_{1s} is plotted against the resonance frequency and the *second acoustic virial coefficient* β can be determined [12]. As an illustrative example, we proceed to analyse the recent data published in our re-determine the Boltzmann constant paper [13].

The fitted A_{1s} coefficients can be represented by:

$$A_{1s} = \frac{\beta_{meas}}{RT} = \frac{\beta + \Delta\beta_{shell}}{RT} \tag{38}$$

Where $\Delta\beta_{shell}$ is the mode dependent shell perturbation that can be modelled as a simple resonance by:

$$\Delta\beta_{shell} = \frac{\kappa}{1 - (f_{0s}\,/f_{breath})^2} \tag{39}$$

Where κ and f_{breath} are a coupling constant and the shell breathing-mode frequency respectively.

Linear regression is used to find the values of κ and f_{breath} such that the value of β is consistent for all modes. Figure 29 shows the results for the sphere used in [13].

a)

Mode (0,s)	f_{0s} / Hz	A_{1s} / kPa^{-1}.m^2.s^{-2}	β_{meas} / cm^3.mol^{-1}	$\Delta\beta$ / cm^3.mol^{-1}	β / cm^3.mol^{-1}
2	3550.4895	0.221588	5.31118	0.13689	5.44807
3	6104.1456	0.220508	5.28529	0.15732	5.44261
4	8615.9451	0.217583	5.21518	0.20269	5.41787
7	16096.485	0.245996	5.89621	-0.45877	5.43744
8	18584.011	0.233861	5.60534	-0.18184	5.42351
9	21070.313	0.231405	5.54648	-0.10761	5.43887
				β_{aver}	**5.438**
				κ	**0.1284**
				f_{breath}	**14.23 kHz**

b)

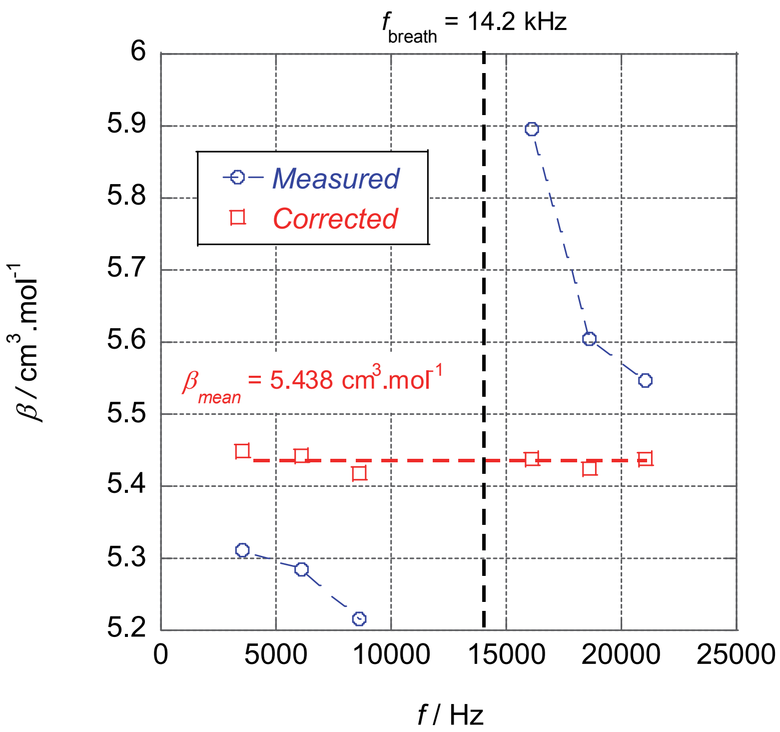

Figure 29 Determination of the second acoustic virial coefficient β and the shell breathing mode frequency.

33. FITTING THE SPEED OF SOUND DATA

Following the convention used in Equation 37, the fitting function for the *speed of sound squared* measurements for an isotherm is typically given by:

$$u_{exp}^2(T,P) = A_0(1 + A_{-1}P^{-1} + A_{1s}P + A_2P^2 + A_3P^3) \tag{40}$$

Where:

$A_{-1}P^{-1}$ accounts for the effect of incomplete thermal accommodation between the gas and the walls of the resonator and must be determined experimentally.
$A_{1s}P$ accounts for the *second acoustic virial coefficient*, β and the mode-dependent shell perturbation.
A_2P^2 accounts for the *third acoustic virial coefficient*, ϕ.
A_3P^3 accounts for the *fourth acoustic virial coefficient*.

For measurements made at T_{TPW} at pressures below 700 kPa, the A_3P^3 term is subtracted before fitting since A_3 can be found in literature with lower uncertainty than it can be measured [13]. At higher pressures and or lower temperatures, it is unclear as to whether good data exists (see Appendix IV) and it may be more prudent to attempt to fit it.

34. CALCULATION OF THE THERMAL ACCOMODATION COEFFICIENT *h*

Once the value of A_{-1} has been determined using Equation 40, the *thermal accommodation coefficient*, h can be calculated. When the acoustic resonance frequencies are corrected for the TBL perturbation, the value of h should be set to 2 in Equation 26. This effectively switches 'off' the *thermal accommodation* correction since $(2-h)/h = 0$, and gives the best contrast for the P^{-1} term allowing A_{-1} to be determined with the lowest possible uncertainty.

$$l_{th} = \frac{\lambda}{P}\left(\frac{\pi MT}{2R}\right)^{0.5}\left(\frac{2-h}{h}\right)\left(\frac{1}{C_V M/R + 1/2}\right) \tag{26*}$$

For a given gas (argon in this case) and a single isotherm, l_{th} is proportional to P^{-1} to good approximation. By way of an example, the value of h for our recent re-determine the Boltzmann constant [13] can be found as follows:

For argon gas at T=273.16 K, Equation 26 can be simplified to:

$$l_{th} \approx 1.1825 \times 10^{-2}\left(\frac{2-h}{h}\right)P^{-1} \tag{41}$$

From Equation 28a, the *thermal accommodation* perturbation is given by:

$$\left(\frac{\Delta f}{f_0}\right)_h = \frac{(\gamma - 1)}{a}l_{th} \tag{42}$$

For a sphere of radius a=0.06201 m and $\gamma \approx 5/3$, the perturbation to u^2 is given by:

$$\left(\frac{\Delta u^2}{u_0^2}\right)_h = 2\left(\frac{\Delta f}{f_0}\right)_h \approx K\left(\frac{2-h}{h}\right)P^{-1} = A_{-1}P^{-1} \tag{43}$$

With K= 0.25426 Pa.
The value of h is therefore given by:

$$h = \frac{2}{1 + \frac{A_{-1}}{K}} \tag{44}$$

Our fitted value of A_{-1} was 0.40 Pa [13] leading to a value of $h = 0.777$[13].

35. CALCULATION OF THE DUCT PERTURBATION: Δ*f*/*f*, *g*/*f*

In order to flow gas into and out of the sphere, ducts of characteristic length and cross-sectional area are used. The method of *equivalent 'T' circuits* [14] is used to model these perturbations. The inlet duct normally consists of two cylindrical ducts in series. The first, attached to the sphere, has a length of L_1 and radius r_1. The second, attached to the first, has a length L_2 and radius r_2. This second duct is normally coiled around the middle of the outside of the sphere many times and then passes to the feed-in pipe work of the pressure vessel. The outlet duct consists of a single tube of length L_1 and radius r_1 and vents directly into the pressure vessel. This is not the same L_1 and $r_1$of the inlet duct but we keep this convention since the two ducts are considered separately in the following formalism. Figures 30 and 31 show the *equivalent T circuits* for the inlet and outlet ducts respectively. For a spherical acoustic resonator, best practice is to select L_1 for the outlet duct equal to the radius of the sphere and L_1 for the inlet ducts equal to twice this length. In doing this, the perturbations are minimised and there is minimal interaction between the two ducts.

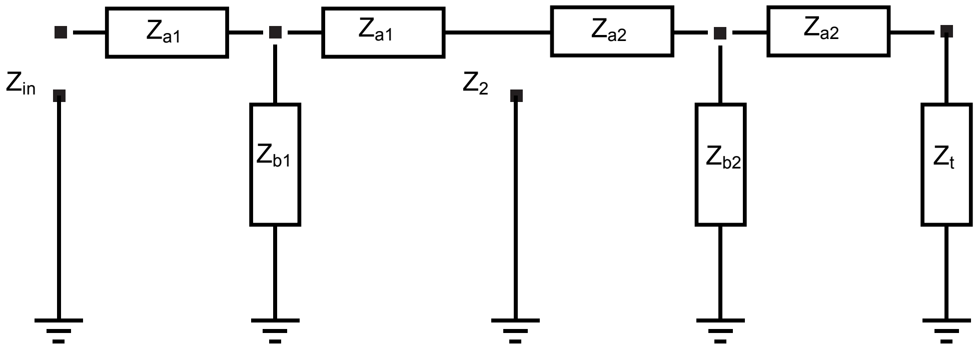

Figure 30 *Equivalent T circuit*: inlet duct – The input impedance is at the inner wall of the sphere and the terminal impedance (Z_t) is at the entry point of the pressure vessel.

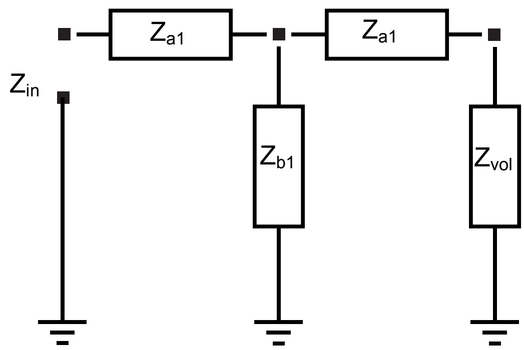

Figure 31 *Equivalent T circuit*: outlet duct – The input impedance is at the inner wall of the sphere and Z_{vol} is the volume impendence of the pressure vessel.

The input impedance of the inlet duct is given by:

$$Z_{in} = Z_{a1} + \frac{(Z_{a1} + Z_2)}{(Z_{a1} + Z_2 + Z_{b1})} Z_{b1} \tag{45}$$

where:

$$Z_2 = Z_{a2} + \frac{(Z_{a2} + Z_t)}{(Z_{a2} + Z_{b2} + Z_t)} Z_{b2} \tag{46}$$

And Z_t is set to 1×10^9 Pa.s.m^{-3} but since the second duct is sufficiently long, changing the value makes little difference.
The input impedance of the outlet duct is given by:

$$Z_{in} = Z_{a1} + \frac{(Z_{a1} + Z_{vol})}{(Z_{a1} + Z_{b1} + Z_{vol})} Z_{b1} \tag{47}$$

With:

$$Z_{vol} = -\frac{i\rho u^2}{2\pi f V_{vessel}} \tag{48}$$

Where:

ρ is the gas density.
f is the frequency.
u is the speed of sound in the gas.
V_{vessel} is the volume of the pressure vessel.

The remaining parameters in Equations 45 to 47 are defined in Equations 49 to 53, where the cross-sectional area of the j^{th} duct is $A_j = \pi r_j^2$, J_v are Bessel functions and δ_v and δ_t are the viscous and thermal penetration lengths respectively.

$$\kappa_v = \frac{1-i}{\delta_v} \qquad \kappa_t = \frac{1-i}{\delta_t} \tag{49a/b}$$

$$F_{vj} = \frac{2J_1(\kappa_v r_j)}{\kappa_v r_j J_0(\kappa_v r_j)} \qquad F_{tj} = \frac{2J_1(\kappa_t r_j)}{\kappa_t r_j J_0(\kappa_t r_j)} \tag{50a/b}$$

$$\Gamma_j = i\left(\frac{2\pi f}{u}\right)\sqrt{\frac{1 + (\gamma - 1)F_{tj}}{1 - F_{vj}}} \tag{51}$$

$$Z_{0j} = \frac{\rho u / A_j}{\sqrt{(1 + (\gamma - 1)F_{tj})(1 - F_{vj})}} \tag{52}$$

$$Z_{aj} = Z_{0j} TANH\left(\frac{\Gamma_j L_j}{2}\right) \qquad Z_{bj} = \frac{Z_{0j}}{SINH\,(\Gamma_j L_j)} \tag{53a/b}$$

Finally, the duct perturbation for the s^{th} radial acoustic mode is given by:

$$\frac{\Delta f_s + i g_s}{f_s} = \frac{i\rho u}{4\pi a^2 Z_s Z_{in}} \tag{54}$$

where: Z_s is the eigenvalue of the mode, Z_{in} is the input impedance of the duct(s) defined in Equations 45 to 47 and a is the radius of the sphere.

Three Labview VI's have been written to calculate the duct perturbations:

1. *Single duct to vessel 2014.vi* – calculates the input impedance, Z_{in} due to the single duct venting to the pressure vessel with terminal impedance Z_{vol}.
2. *Two ducts to Zt 2014.vi* – calculates the input impedance, Z_{in} due to the two joined ducts with terminal impedance Z_t.
3. *Duct pert full argon 2014.vi* – calculates the perturbations $\Delta f/f$ and g/f for argon gas for a given T, P and a due to the inlet and outlet duct(s) whose input impedances are given by the VI's described in 1. and 2. above. The data is also available on the clipboard for use in Excel etc.

Figure 32 shows the three Labview VI's.

a)

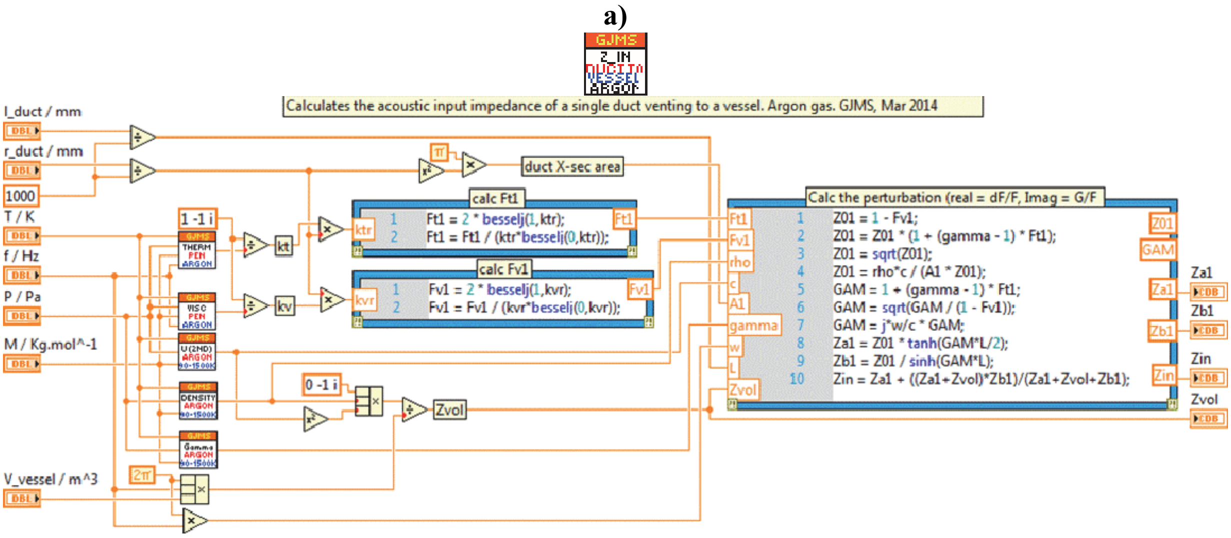

b)

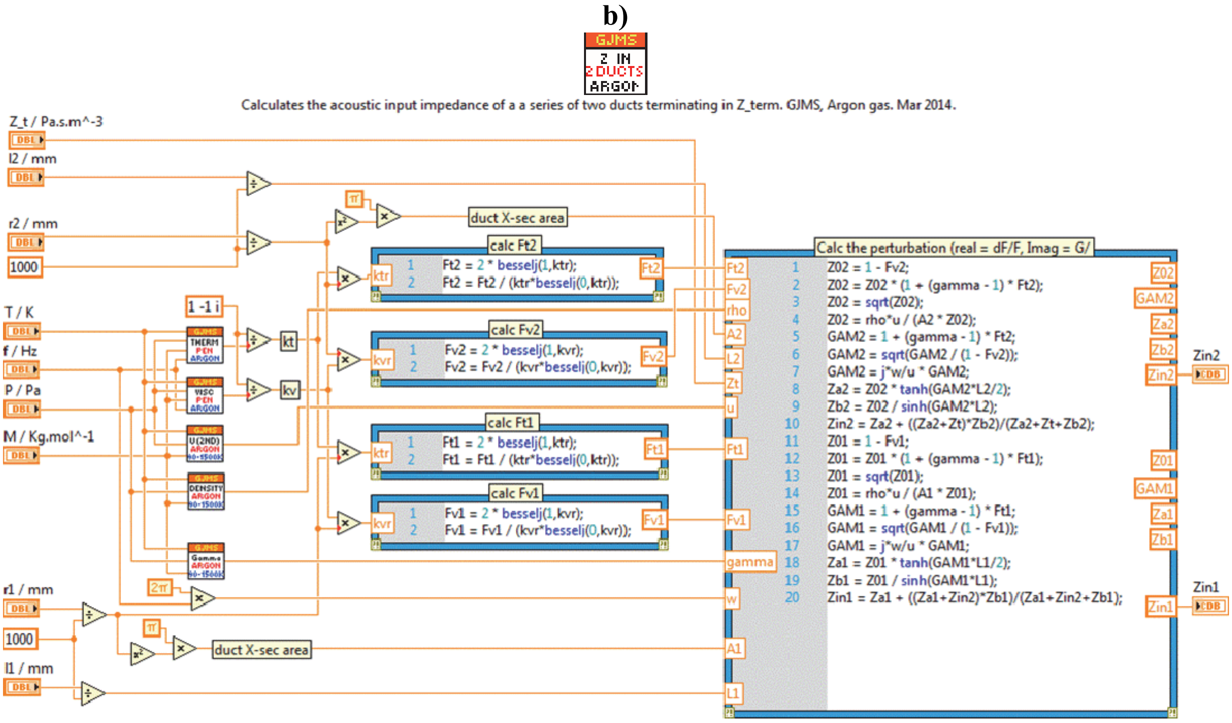

c)

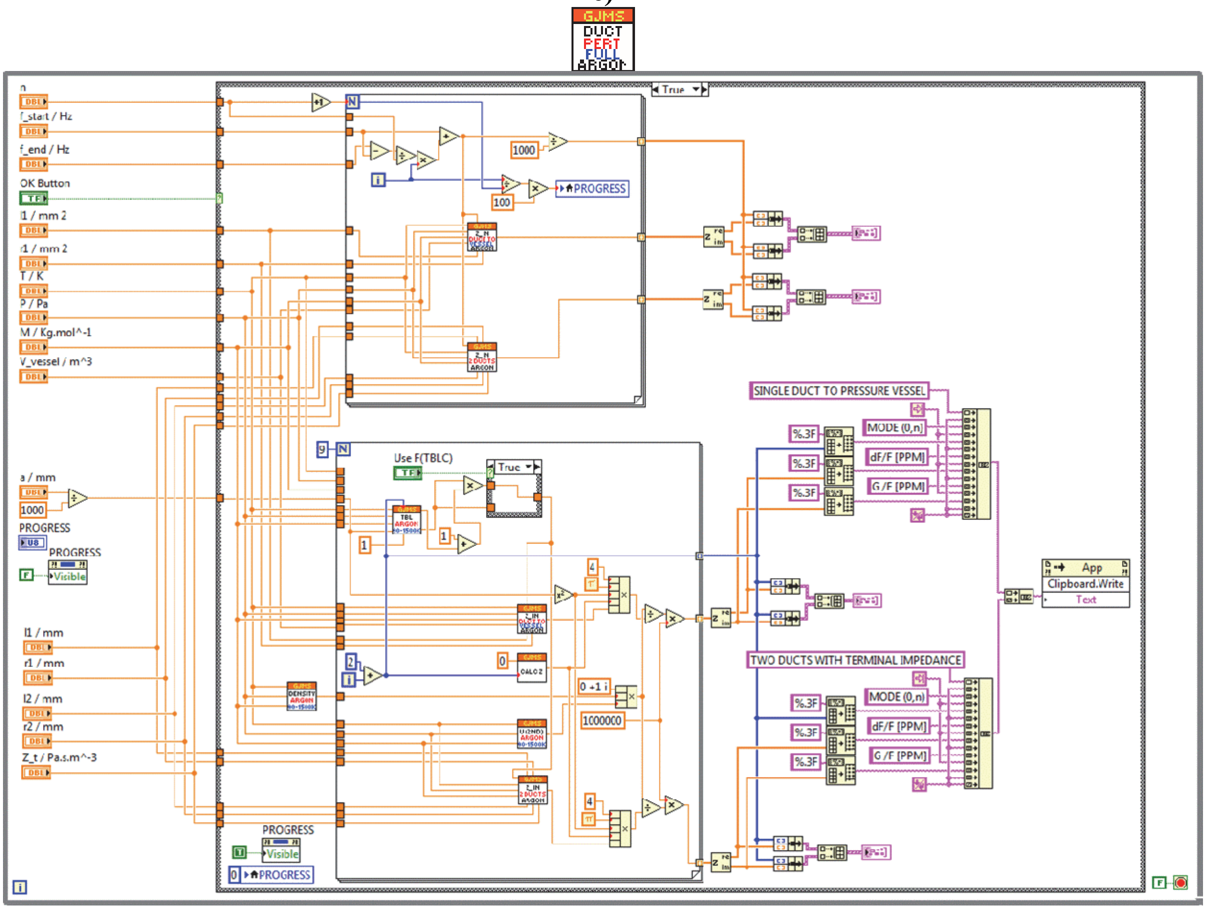

Figure 32 Duct perturbations: *Equivalent T circuit* method: Labview VI's: a) *duct to vessel 2014.vi*, b) *Two ducts to Zt 2014.vi* and c) *Duct pert full argon 2014.vi*.

As an example, the duct perturbation for the NPL sphere used in the recent re-determination of the Boltzmann constant [13] is calculated. The duct parameters are given in Table 4 and the perturbation is calculated at three temperatures (T = 173.15 K, T = 273.16 K and T = 373.15 K) for pressures from 20 kPa to 600 kPa and for the first 9 radial modes. Figures 33, 34 and 35 show these calculations for the inlet, outlet and combined ducts.

a / mm	62.01	***T* / K**	173.15, 273.16, 373.15
M / kg.mol^{-1}	0.0399478		
Inlet ducts:		**Outlet duct:**	
L_1 / mm	124	L_1 / mm	62
r_1 / mm	0.317	r_1 / mm	0.261
L_2 / mm	6000	V_{vessel} / m^3	0.012
r_2 / mm	0.45		
Z_t / Pa.s.m^{-3}	1.00E+09		

Table 4 Duct parameters for the NPL sphere [13].

a) T = 173.15 K

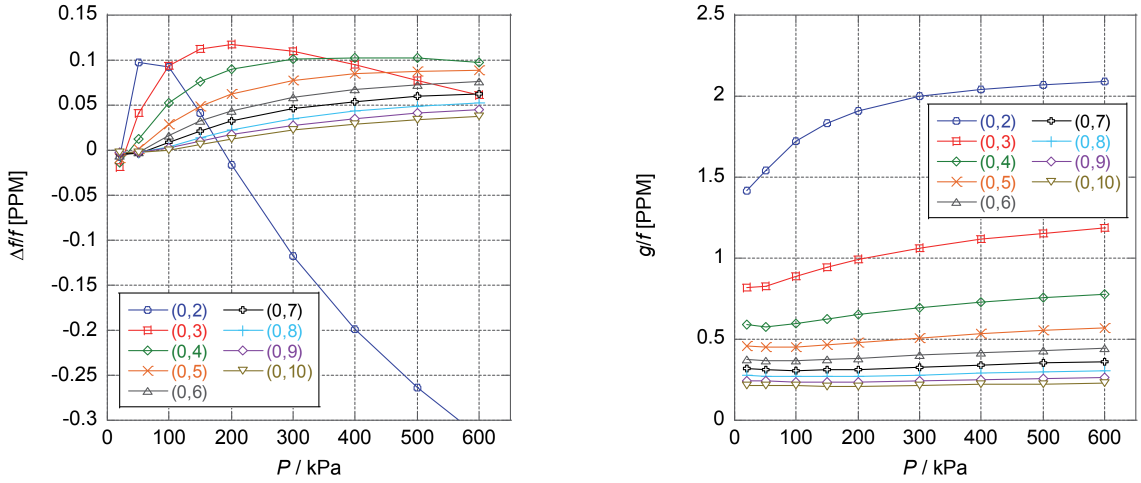

b) T = 273.16 K

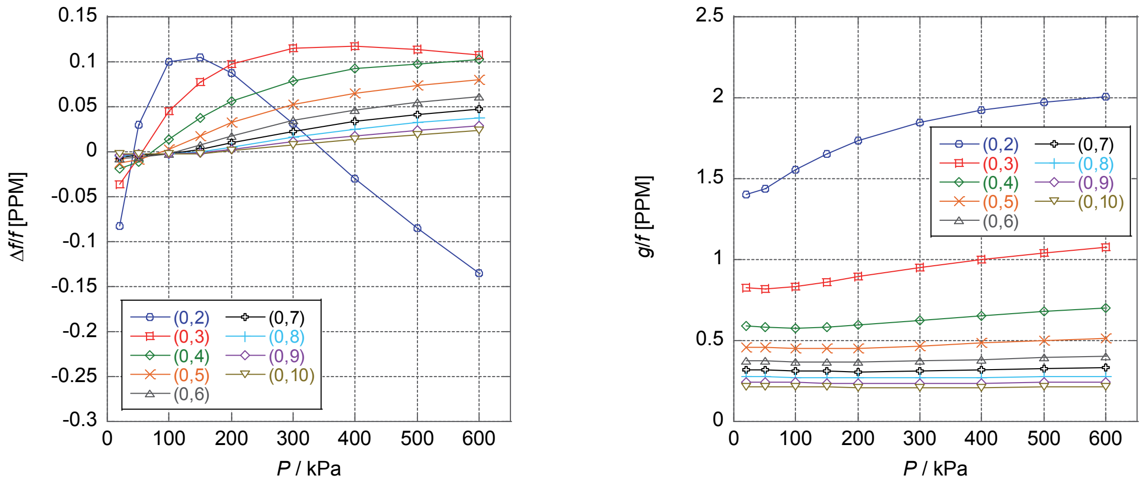

c) T = 373.15 K

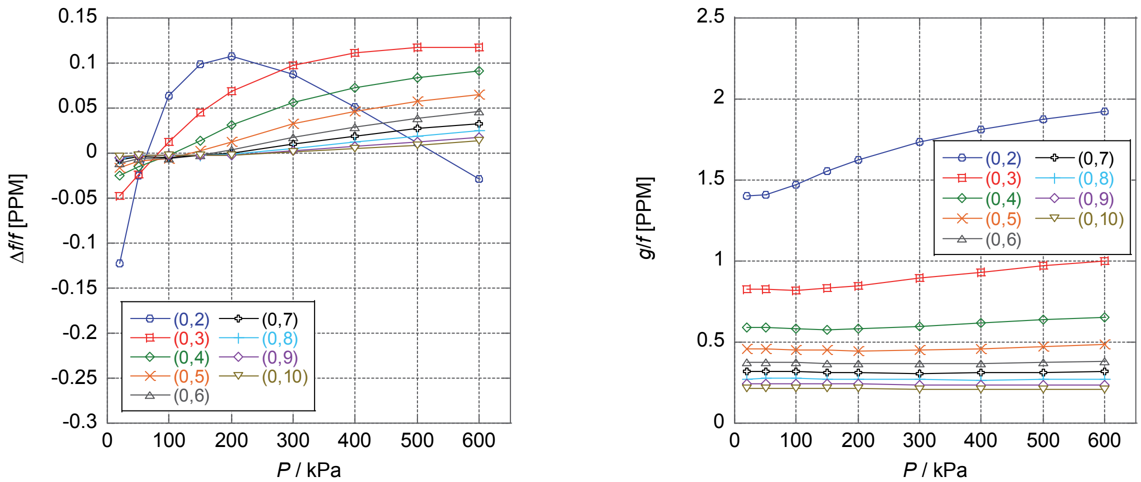

Figure 33 Duct perturbation for the NPL sphere [13]: Inlet ducts.

a) *T* = 173.15 K

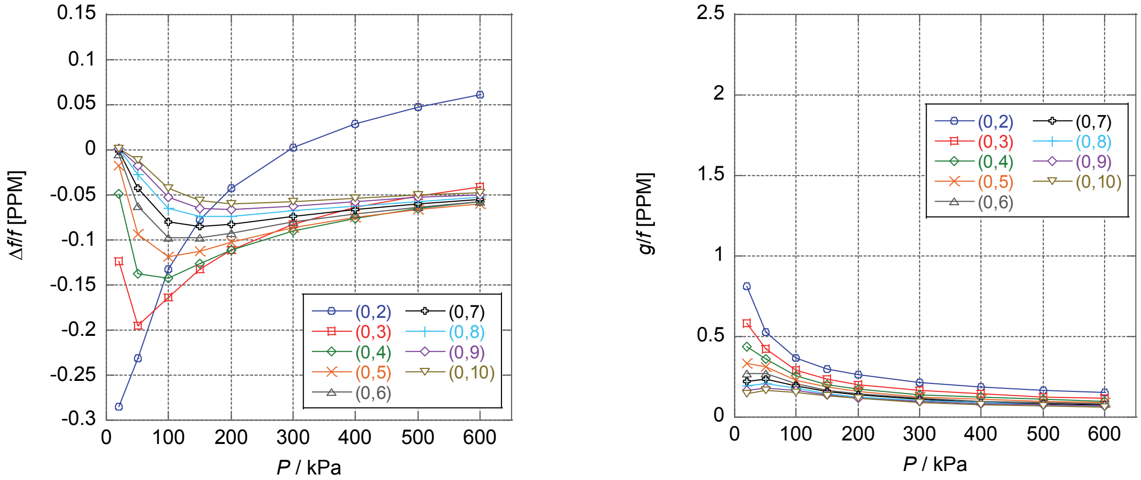

b) *T* = 273.16 K

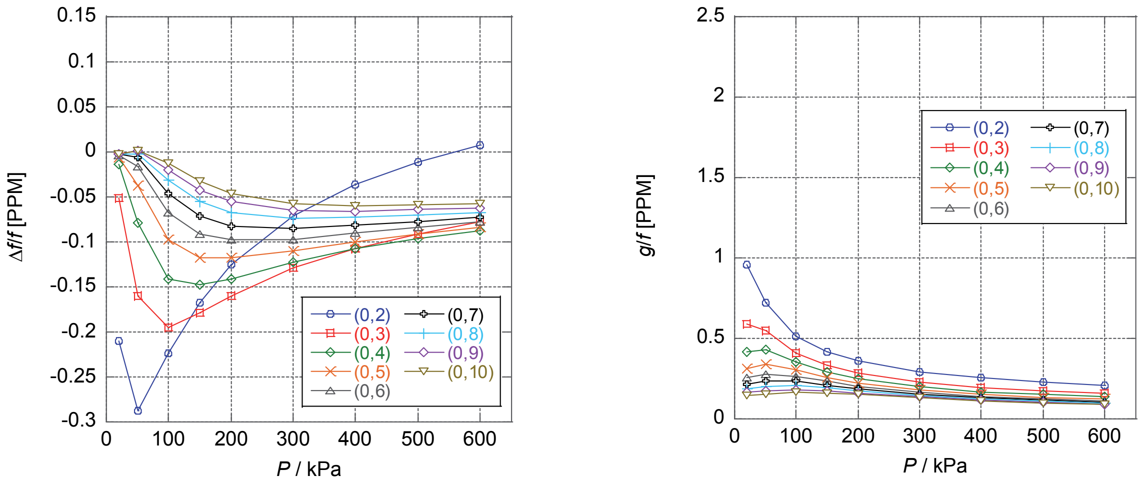

c) *T* = 373.15 K

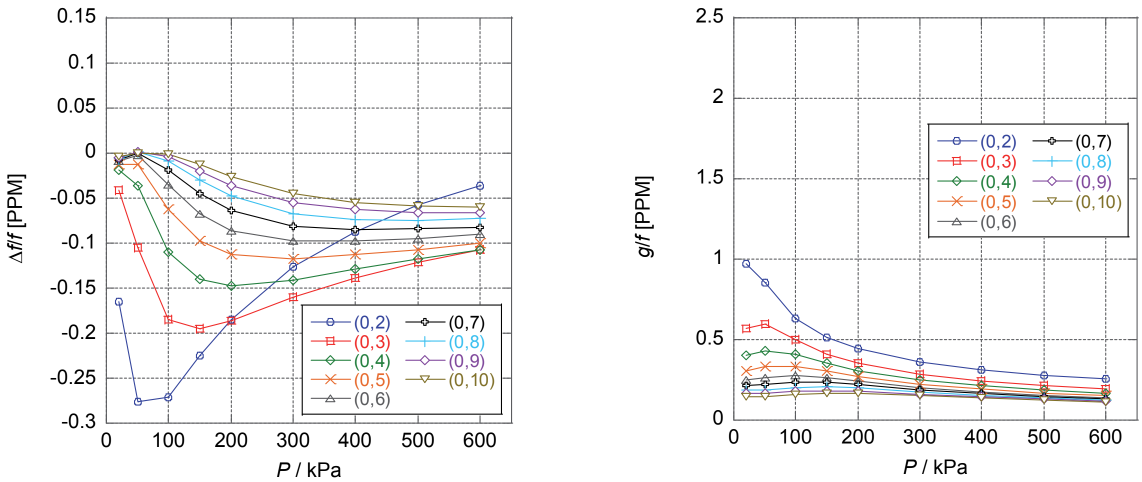

Figure 34 Duct perturbation for the NPL sphere [13]: Outlet duct.

a) *T* = 173.15 K

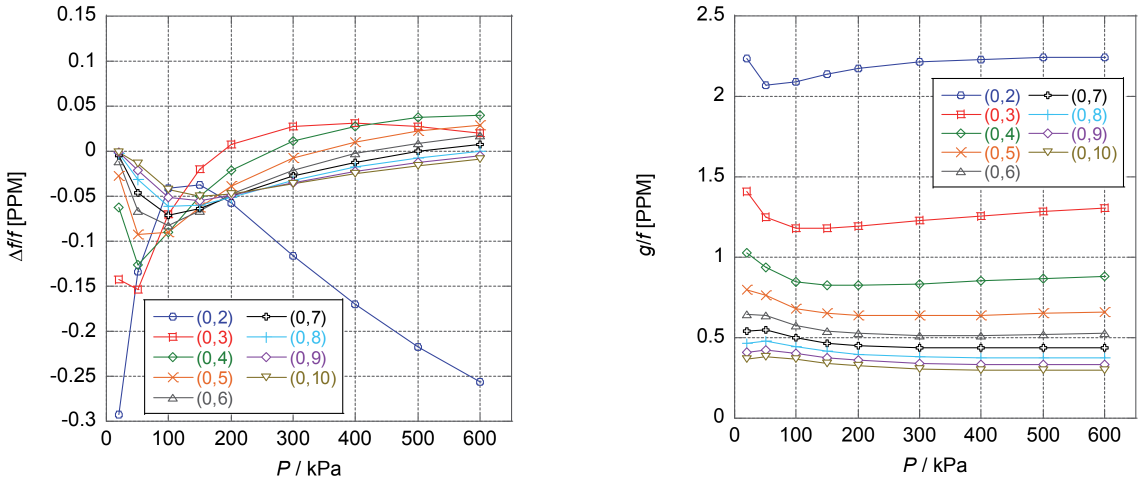

b) *T* = 273.16 K

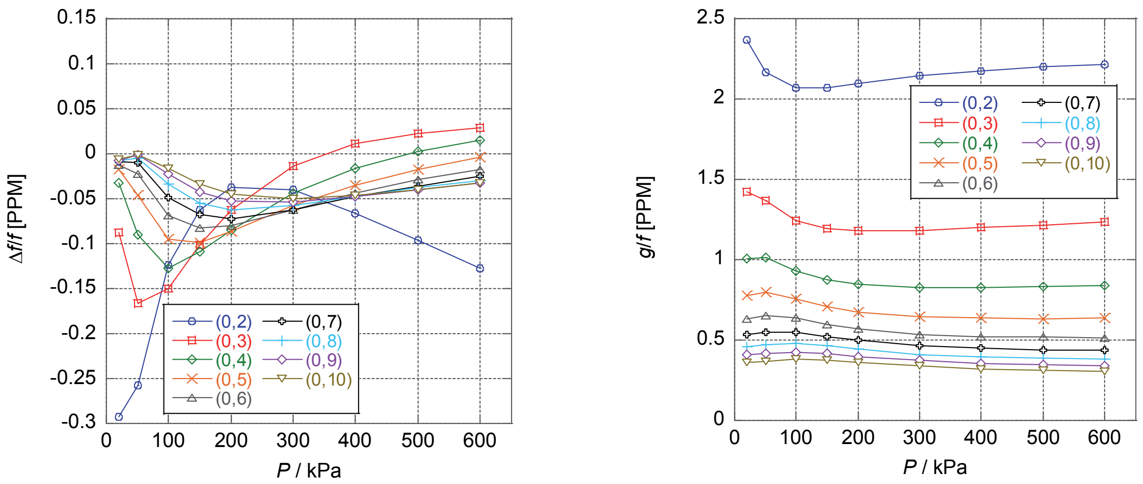

c) *T* = 373.15 K

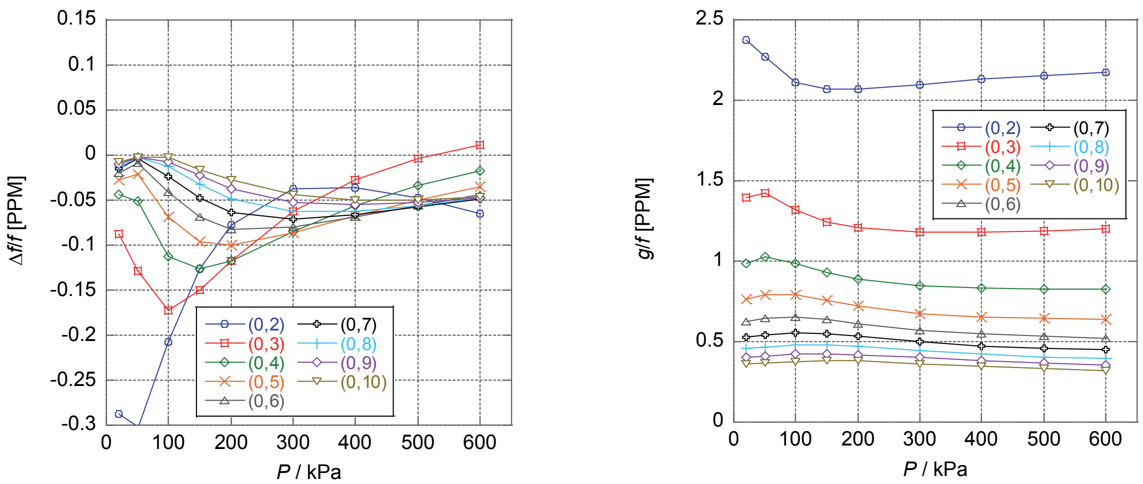

Figure 35 Duct perturbation for the NPL sphere [13]: Combined Inlet and outlet ducts.

References

[1] *Handbook of the speed of sound in real gases – Volume 1*, A. J. Zuckerwar, Academic Press 2002.

[2] *Acoustic gas thermometry*, M. R. Moldover, R. M. Gavioso, J. B. Mehl, L. Pitre, M de Podesta, J. T. Zhang, Metrologia **51** (2014), R1 – R19.

[3] *Ab initio virial equation of state for argon using a new nonadditive three-body potential*, B. Jäger, R. Hellmann, E. Bich, E. Vogel, J. Chem. Phys. **135** 084308 (2011).

[4] *NIST Standard Reference Database 23: Reference Fluid Thermodynamic and Transport Properties- REFPROP*, E. W. Lemmon, M. L. Huber, M. O. McLinden, Version 9.1, National Institute of Standards and Technology, Standard Reference Data Program, Gaithersburg, 2013.

[5] *Determination of the Boltzmann constant: acoustic models and corrections for argon and helium*, G. Sutton, NPL Report ENG 19 (2009).

[6] *Thermal Conductivity of Selected Materials*, R. W. Powell, C. Y. Ho and P. E. Liley, http://www.nist.gov/data/nsrds/NSRDS-NBS-8.pdf. 1966.

[7] *Heat Capacity of Reference Materials: Cu and W*, G. K. White and S. J. Collocott, J. Phys. Chem. Ref. Data **13**, 4, 1984.

[8] *Second-order boundary corrections to the radial acoustic eigenvalues for a spherical cavity*, K. A. Gillis, Metrologia **49**, (2012) L21-L24.

[9] *Acoustic eigenvalues of a quasi-spherical resonator: second order shape perturbation theory for arbitrary modes*, J. B. Mehl, J. Res. Natl. Inst. Stand. Technol. 122, 163-173 (2007).

[10] *The speed of sound in gaseous argon at temperatures between 110 K and 450 K and at pressures up to 19 MPa*, A. F. Estrada-Alexanders, J. P. M. Trusler, J. Chem Thermodynamics **27** (1995), 1075-1089.

[11] *Sensitivity of the thermal and acoustic virial coefficients of argon to the argon interaction potential*, J. Wiebke, E. Pahl, P. Schwerdtfeger, J. Chem. Phys. **137** (2012), 064702.

[12] *Acoustic thermometry: new results from 273K to 77K and progress towards 4K*, L. Pitre, M. R. Moldover and W. L. Tew, Metrologia 43 142–62 (2006).

[13] *A low-uncertainty measurement of the Boltzmann constant*, M. dePodesta, R. Underwood, G. Sutton, P. Morantz, P. Harris, D. Mark, F. Stuart, G. Vargha, G. Machin, Metrologia **50** (2013) 354-376.

[14] *Designing quasi-spherical resonators for acoustic thermometry*, J. B. Mehl, M. R. Moldover, L. Pitre, Metrologia **41** (2004) 295 – 304.

[15] *Thermophysical Properties from the Speed of Sound*, A. R. H. Goodwin, Ph.D. Thesis, University of London (1988).

Appendix 1 – Thermophysical Properties of argon

Supplement B: Calculated Properties of Argon at Zero Density

From *Acoustic gas thermometry*, M. R. Moldover et al, Metrologia 51(2014) R1 [2]

T	B	β	η	λ	$U(B)$; $k=2$	$U(\beta)$; $k=2$	$U(\eta)$; $k=2$	$U(\lambda)$; $k=2$
K	cm^3/mol	cm^3/mol	μPa s	mWK^{-1}m^{-1}	cm^3/mol	cm^3/mol	μPa s	mWK^{-1}m^{-1}
80	-276.552	-300.696	6.56691	5.12691	1.68E+00	2.30E+00	6.21E-03	4.84E-03
82	-263.775	-283.719	6.72121	5.24723	1.59E+00	2.15E+00	6.39E-03	4.98E-03
84	-251.954	-268.195	6.87603	5.36795	1.51E+00	2.03E+00	6.58E-03	5.12E-03
86	-240.988	-253.95	7.03133	5.48905	1.44E+00	1.91E+00	6.75E-03	5.26E-03
88	-230.789	-240.835	7.18707	5.61051	1.37E+00	1.81E+00	6.93E-03	5.40E-03
90	-221.282	-228.722	7.34323	5.7323	1.31E+00	1.72E+00	7.10E-03	5.53E-03
92	-212.4	-217.502	7.49977	5.85439	1.26E+00	1.63E+00	7.26E-03	5.66E-03
94	-204.086	-207.082	7.65666	5.97676	1.21E+00	1.55E+00	7.43E-03	5.79E-03
96	-196.286	-197.381	7.81386	6.09938	1.16E+00	1.48E+00	7.58E-03	5.91E-03
98	-188.957	-188.326	7.97134	6.22223	1.11E+00	1.42E+00	7.73E-03	6.03E-03
100	-182.057	-179.856	8.12907	6.34528	1.07E+00	1.36E+00	7.88E-03	6.15E-03
105	-166.462	-160.896	8.52429	6.65362	9.81E-01	1.23E+00	8.23E-03	6.42E-03
110	-152.871	-144.579	8.92038	6.96268	9.04E-01	1.13E+00	8.55E-03	6.67E-03
115	-140.928	-130.391	9.31693	7.27211	8.37E-01	1.04E+00	8.83E-03	6.90E-03
120	-130.355	-117.941	9.71351	7.5816	7.80E-01	9.63E-01	9.09E-03	7.10E-03
125	-120.932	-106.929	10.10978	7.89087	7.29E-01	8.97E-01	9.32E-03	7.27E-03
130	-112.485	-97.1228	10.50539	8.19964	6.85E-01	8.41E-01	9.51E-03	7.43E-03
135	-104.87	-88.3342	10.90005	8.5077	6.46E-01	7.91E-01	9.68E-03	7.56E-03
140	-97.9737	-80.4104	11.2935	8.81483	6.11E-01	7.49E-01	9.82E-03	7.67E-03
145	-91.6992	-73.2349	11.68551	9.12086	5.80E-01	7.10E-01	9.94E-03	7.77E-03
150	-85.9675	-66.7057	12.07587	9.42562	5.52E-01	6.76E-01	1.00E-02	7.84E-03
155	-80.7122	-60.7398	12.46441	9.72899	5.26E-01	6.45E-01	1.01E-02	7.89E-03
160	-75.877	-55.2681	12.85098	10.03084	5.03E-01	6.17E-01	1.01E-02	7.93E-03
165	-71.4144	-50.232	13.23544	10.33107	4.82E-01	5.92E-01	1.02E-02	7.95E-03
170	-67.2834	-45.5826	13.61768	10.62959	4.63E-01	5.69E-01	1.02E-02	7.96E-03
175	-63.4491	-41.2774	13.9976	10.92634	4.45E-01	5.48E-01	1.02E-02	7.95E-03
180	-59.8811	-37.2801	14.37514	11.22124	4.29E-01	5.29E-01	1.01E-02	7.93E-03
185	-56.553	-33.5597	14.75022	11.51426	4.14E-01	5.11E-01	1.01E-02	7.90E-03
190	-53.4419	-30.0883	15.12279	11.80535	4.00E-01	4.94E-01	1.00E-02	7.86E-03
195	-50.5276	-26.8426	15.49281	12.09447	3.87E-01	4.79E-01	9.93E-03	7.80E-03
200	-47.7923	-23.8011	15.86025	12.38162	3.74E-01	4.65E-01	9.85E-03	7.74E-03
205	-45.2202	-20.9469	16.22509	12.66676	3.63E-01	4.51E-01	9.75E-03	7.66E-03
210	-42.7976	-18.263	16.58731	12.9499	3.52E-01	4.39E-01	9.64E-03	7.58E-03
215	-40.512	-15.7349	16.94691	13.23102	3.42E-01	4.27E-01	9.52E-03	7.49E-03
220	-38.3523	-13.3493	17.3039	13.51012	3.33E-01	4.17E-01	9.39E-03	7.40E-03
225	-36.3086	-11.0955	17.65826	13.78721	3.24E-01	4.06E-01	9.25E-03	7.30E-03
230	-34.372	-8.96287	18.01001	14.06229	3.16E-01	3.96E-01	9.11E-03	7.19E-03
235	-32.5346	-6.94214	18.35917	14.33537	3.08E-01	3.87E-01	8.96E-03	7.08E-03
240	-30.789	-5.02664	18.70576	14.60647	3.01E-01	3.79E-01	8.81E-03	6.97E-03
245	-29.1286	-3.20653	19.04978	14.87561	2.94E-01	3.71E-01	8.65E-03	6.85E-03

250	-27.5477	-1.47569	19.39127	15.14279	2.87E-01	3.63E-01	8.49E-03	6.73E-03
260	-24.6025	1.74086	20.06676	15.67138	2.75E-01	3.49E-01	8.17E-03	6.48E-03
270	-21.9158	4.66778	20.73243	16.19242	2.63E-01	3.36E-01	7.84E-03	6.23E-03
280	-19.4556	7.33928	21.38854	16.70608	2.53E-01	3.24E-01	7.50E-03	5.98E-03
290	-17.1952	9.78655	22.03535	17.21256	2.44E-01	3.13E-01	7.18E-03	5.73E-03
300	-15.1121	12.03634	22.67312	17.71208	2.35E-01	3.03E-01	6.87E-03	5.49E-03
310	-13.1866	14.10805	23.30213	18.20483	2.27E-01	2.94E-01	6.58E-03	5.27E-03
320	-11.4021	16.02292	23.92266	18.69102	2.20E-01	2.85E-01	6.32E-03	5.06E-03
330	-9.74414	17.79666	24.53498	19.17086	2.13E-01	2.77E-01	6.09E-03	4.87E-03
340	-8.20022	19.44303	25.13935	19.64456	2.07E-01	2.70E-01	5.89E-03	4.71E-03
350	-6.75935	20.97453	25.73605	20.11231	2.01E-01	2.63E-01	5.74E-03	4.58E-03
360	-5.41194	22.40203	26.32533	20.57431	1.96E-01	2.57E-01	5.63E-03	4.48E-03
370	-4.14953	23.73509	26.90744	21.03075	1.90E-01	2.51E-01	5.58E-03	4.42E-03
380	-2.96464	24.98187	27.48262	21.48182	1.86E-01	2.45E-01	5.58E-03	4.40E-03
390	-1.85064	26.14988	28.05111	21.92769	1.81E-01	2.40E-01	5.62E-03	4.42E-03
400	-0.80163	27.24611	28.61313	22.36853	1.77E-01	2.35E-01	5.72E-03	4.48E-03
410	0.18766	28.27666	29.16891	22.80452	1.73E-01	2.30E-01	5.87E-03	4.57E-03
420	1.12195	29.24525	29.71865	23.23581	1.69E-01	2.26E-01	6.06E-03	4.69E-03
430	2.00548	30.15825	30.26255	23.66255	1.65E-01	2.21E-01	6.29E-03	4.85E-03
440	2.84207	31.01934	30.8008	24.0849	1.62E-01	2.17E-01	6.55E-03	5.04E-03
450	3.63517	31.83255	31.3336	24.50299	1.59E-01	2.14E-01	6.84E-03	5.24E-03
460	4.38792	32.60166	31.86111	24.91695	1.56E-01	2.10E-01	7.15E-03	5.47E-03
470	5.10313	33.32919	32.38351	25.32693	1.53E-01	2.06E-01	7.48E-03	5.72E-03
480	5.78339	34.01837	32.90095	25.73304	1.50E-01	2.03E-01	7.83E-03	5.98E-03
490	6.43106	34.6714	33.41361	26.13541	1.47E-01	2.00E-01	8.20E-03	6.25E-03
500	7.04827	35.29158	33.92161	26.53415	1.45E-01	1.97E-01	8.57E-03	6.53E-03
520	8.19903	36.44008	34.92426	27.32116	1.40E-01	1.91E-01	9.35E-03	7.12E-03
540	9.24955	37.47903	35.90996	28.09492	1.35E-01	1.86E-01	1.01E-02	7.73E-03
560	10.21154	38.42065	36.87969	28.85617	1.31E-01	1.81E-01	1.10E-02	8.35E-03
580	11.09501	39.27905	37.83438	29.60562	1.28E-01	1.78E-01	1.18E-02	8.98E-03
600	11.90851	40.05934	38.77484	30.34391	1.24E-01	1.73E-01	1.26E-02	9.61E-03
620	12.65944	40.77409	39.70184	31.07164	1.21E-01	1.67E-01	1.34E-02	1.02E-02
640	13.35418	41.42929	40.61608	31.78935	1.18E-01	1.64E-01	1.42E-02	1.09E-02
660	13.99831	42.03308	41.51822	32.49755	1.15E-01	1.61E-01	1.50E-02	1.15E-02
680	14.59668	42.57997	42.40886	33.1967	1.12E-01	1.60E-01	1.58E-02	1.21E-02
700	15.15359	43.08644	43.28856	33.88725	1.10E-01	1.54E-01	1.66E-02	1.27E-02
720	15.67279	43.54793	44.15783	34.5696	1.08E-01	1.52E-01	1.74E-02	1.33E-02
740	16.15762	43.98344	45.01715	35.24411	1.05E-01	1.49E-01	1.81E-02	1.39E-02
760	16.61104	44.37937	45.86697	35.91114	1.03E-01	1.51E-01	1.89E-02	1.45E-02
780	17.03569	44.74587	46.7077	36.57102	1.01E-01	1.45E-01	1.97E-02	1.51E-02
800	17.43393	45.08326	47.53973	37.22404	9.95E-02	1.43E-01	2.04E-02	1.57E-02
820	17.80787	45.39711	48.36343	37.87049	9.77E-02	1.40E-01	2.11E-02	1.63E-02
840	18.15941	45.68989	49.17912	38.51064	9.60E-02	1.39E-01	2.18E-02	1.68E-02
860	18.49026	45.95195	49.98714	39.14473	9.44E-02	1.33E-01	2.26E-02	1.74E-02
880	18.80197	46.20344	50.78776	39.773	9.29E-02	1.34E-01	2.33E-02	1.79E-02
900	19.09593	46.43278	51.58128	40.39566	9.14E-02	1.37E-01	2.40E-02	1.85E-02

920	19.37342	46.63691	52.36796	41.01293	9.00E-02	1.32E-01	2.46E-02	1.90E-02
940	19.63559	46.84651	53.14804	41.625	8.86E-02	1.28E-01	2.53E-02	1.96E-02
960	19.88349	47.03383	53.92175	42.23204	8.74E-02	1.28E-01	2.60E-02	2.01E-02
980	20.1181	47.19871	54.68932	42.83423	8.61E-02	1.25E-01	2.66E-02	2.06E-02
1000	20.34028	47.3608	55.45095	43.43175	8.49E-02	1.22E-01	2.73E-02	2.11E-02
1050	20.84652	47.69632	57.3303	44.90603	8.22E-02	1.18E-01	2.89E-02	2.24E-02
1100	21.29092	47.98526	59.17653	46.35417	7.97E-02	1.19E-01	3.05E-02	2.36E-02
1150	21.68239	48.23287	60.99208	47.77811	7.74E-02	1.14E-01	3.20E-02	2.48E-02
1200	22.02827	48.4039	62.77911	49.17956	7.53E-02	1.11E-01	3.35E-02	2.60E-02
1250	22.33466	48.55502	64.53955	50.56002	7.33E-02	1.07E-01	3.49E-02	2.71E-02
1300	22.60665	48.67981	66.2751	51.92085	7.15E-02	1.00E-01	3.63E-02	2.82E-02
1350	22.84853	48.77211	67.98729	53.26325	6.98E-02	1.04E-01	3.77E-02	2.93E-02
1400	23.06395	48.84186	69.67751	54.58833	6.83E-02	1.13E-01	3.91E-02	3.04E-02
1450	23.256	48.87058	71.34701	55.89706	6.68E-02	9.58E-02	4.04E-02	3.14E-02
1500	23.42735	48.91386	72.99691	57.19034	6.55E-02	9.80E-02	4.17E-02	3.24E-02

Appendix II – Datafile and Lab View VI's location

1. *Desktop\Boltzmann constant project\Experimental\Acoustics\SOFTWARE\Models and corrections for argon 90K-1500K*
2. *T:\PUBLIC\GJMS\Models and corrections for argon 90K-1500K*

Appendix III – Parameters used to calculate the third density virial coefficient of argon, C [3].

k	$c_{3,k}$ /cm^6.mol^{-2}
-9	0.00000000000E+00
-8	-2.59962699927E-05
-7	9.71352136025E-05
-6	4.01081195695E-03
-5	-1.88028806073E-01
-4	1.64722353365E+00
-3	-1.01735017150E+01
-2	1.37319632897E+02
-1	-9.06798523084E+02
0	-1.34839966042E+02
1	0.00000000000E+00
2	0.00000000000E+00
3	0.00000000000E+00
0.5	3.17008319513E+00
-0.5	1.60786304709E+03

Apendix IV - Variability in the literature value of the third acoustic virial coefficient for argon

To third-order in pressure, the *speed of sound squared* can be written as:

$$u^2(T,p) = \frac{\gamma_0 RT}{M}(1 + A_1 p + A_2 p^2 + A_3 P^3) \tag{A-1}$$

Where:

γ_0 is the ratio of specific heats C_p/C_v in the limit of zero pressure.
R is the molar gas constant.
T is the temperature.
M is the molar mass of the gas.
p is the pressure.

and $$A_1 = \frac{\beta}{RT} \quad , \quad A_2 = \frac{\phi}{(RT)^2} = \frac{L - B\beta}{(RT)^2} \tag{A-2}$$

β and ϕ are known as the *second* and *third acoustic virial coefficients* respectively.

with $$\beta = 2B + 2(\gamma_0 - 1)T\frac{dB}{dT} + \frac{(\gamma_0 - 1)^2}{\gamma_0}T^2\frac{d^2B}{dT^2} \tag{A-3a}$$

and $$L = \left[B + (2\gamma_0 - 1)T\frac{dB}{dT} + (\gamma_0 - 1)T^2\frac{d^2B}{dT^2}\right]^2\left(\frac{\gamma_0 - 1}{\gamma_0}\right) + \left(\frac{1 + 2\gamma_0}{\gamma_0}\right)C + \left(\frac{\gamma_0^2 - 1}{\gamma_0}\right)T\frac{dC}{dT} + \frac{(\gamma_0 - 1)^2}{2\gamma_0}T^2\frac{d^2C}{dT^2} \tag{A-3b}$$

B and C are the *second* and *third density virial coefficients*.

Agreement between literature values of the *second acoustic virial coefficient* β is excellent. Figure A1a) shows the agreement between the values obtained from *Moldover et al* [2], *REFPROP* [4] and Estrada-*Alexanders et al* [10].

Agreement between literature values of the *third acoustic virial coefficient* ϕ is reasonable over the temperature range: 250 K < T < 450 K. However, below 250 K, there are large differences. Figure A1 b) shows a comparison between the values reported by the authors listed above [2, 4, 10] and an additional recent author, *Wiebke et al* [11]. It is not believed that the variability in the reported value of ϕ at low temperatures will cause difficulties in acoustic gas thermometry, since A_2 is usually measured (fitted).

However, a robust estimate of the *fourth acoustic virial* may be needed to determine contributions due to the A_3P^3 term. When determining the Boltzmann constant (at 273.16 K), A_3 is usually taken from literature [15], but at lower temperatures, it may be possible to determine it experimentally.

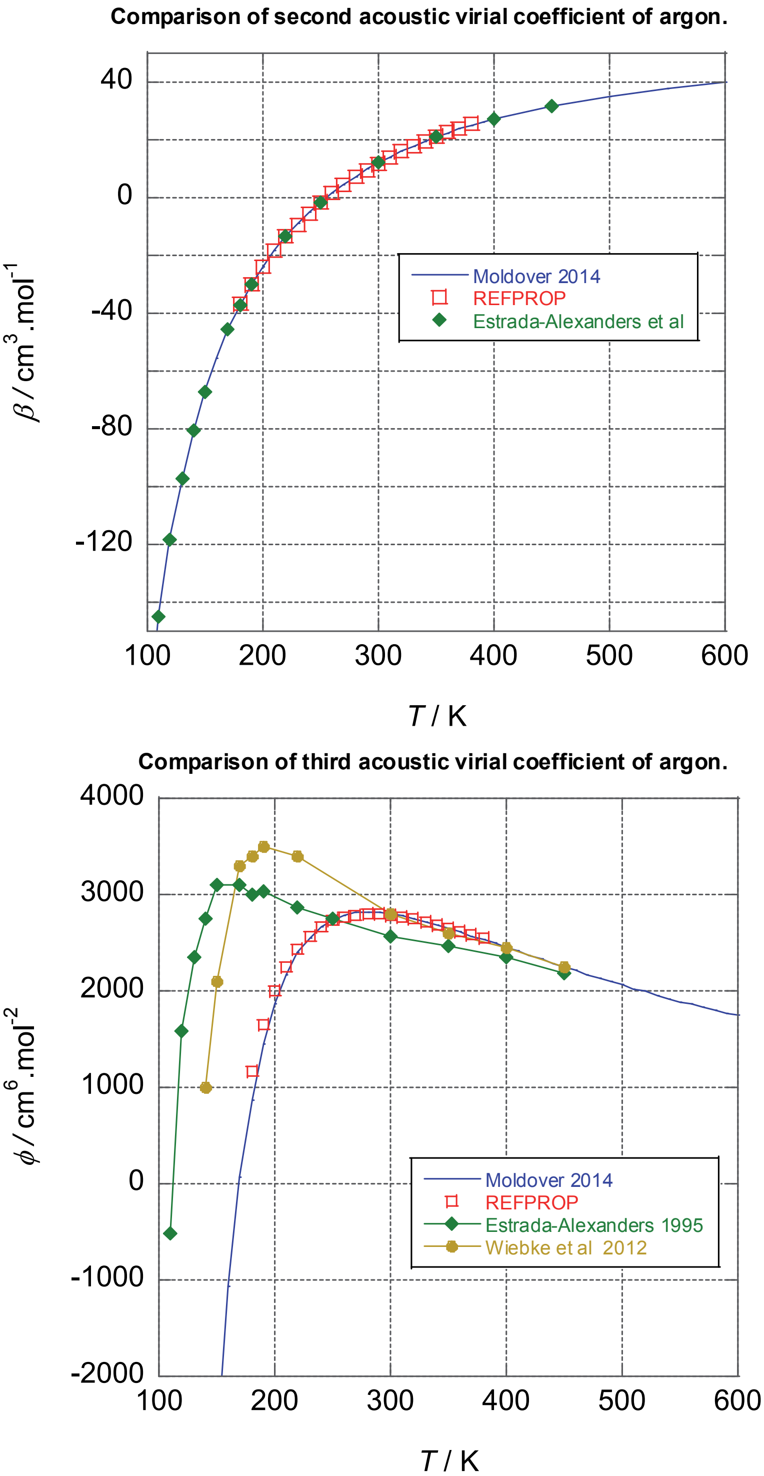

Figure A1 The a) *second* and b) *third acoustic virial coefficients* of argon.